

**The Effect of Sand Gradation on the
Hydro-mechanical Characteristics of Sand-bentonite
Mixtures as Buffer Material**

Soheil Ghadr

Submitted to the
Institute of Graduate Studies and Research
in partial fulfillment of the requirements for the Degree of

Master of Science
in
Civil Engineering

Eastern Mediterranean University
January 2013
Gazimağusa, North Cyprus

Approval of the Institute of Graduate Studies and Research

Prof. Dr. Elvan Yılmaz
Director

I certify that this thesis satisfies the requirements as a thesis for the degree of Master of Science in Civil Engineering.

Asst. Prof. Dr. Mürüde Çelikağ
Chair, Department of Civil Engineering

We certify that we have read this thesis and that in our opinion it is fully adequate in scope and quality as a thesis for the degree of Master of Science in Civil Engineering.

Asst. Prof. Dr. Huriye Bilsel
Supervisor

Examining Committee

1. Prof. Dr. Özgür Eren

2. Assoc. Prof. Dr. Zalihe Sezai

3. Asst. Prof. Dr. Huriye Bilsel

ABSTRACT

Municipal solid waste produces gas, heat and leachate in landfill repository systems. In radioactive waste disposals, radionuclide wastes raise the temperature around the containers as well as applying high pressures on waste barriers which create mechanical stresses that have made them subject to research for determination of hydro-mechanical properties, which are as essential as the thermal properties.

In this thesis, the findings of a study on hydro-mechanical characteristics of compacted sand-bentonite mixtures are presented, which are among the materials recommended to be used as hazardous waste container and barrier materials for landfills as a liner. Mixtures of bentonite with two different types of sand in two different proportions of bentonite (15%-25%) have been studied. The experimental work achieved to assess the characteristics of these mixtures consists of compaction tests, unconfined compression tests, one-dimensional swell-consolidation tests, shrinkage tests and determination of soil-water characteristic curves by suction measurements.

The experimental data obtained in this research study conclude that with increasing bentonite content in mixtures, swelling pressures increased and cracking appeared in samples upon shrinkage, which made the structures unstable. On the other hand saturated hydraulic conductivity and unconfined compressive strength characteristics of mixtures were improved. The changes in hydro-mechanical performance due to various specimen combinations were considered and discussed based on the suction components of soil mixture. At the end, it was concluded that the compacted crushed

limestone sand-bentonite mixture with 15% bentonite content could be a feasible mixture in waste containers as a buffer material which can be considered in future.

Keywords: Compacted sand-bentonite mixtures, hydro mechanical properties, waste containers, landfills

ÖZ

Bu tez çalışmasında zehirli atıkların depolanmasında ve atık depolama sistemlerinde kullanılması öngörülen malzemeler arasında olan sıkıştırılmış kum-bentonit karışımlarının hidro-mekanik davranışının deneysel bulguları sunulmuştur. İki farklı kum türü (deniz ve dağ kumu) ve gradasyonu (SP ve SW) ile iki farklı bentonit miktarının karışımları çalışılmıştır. Bu karışımların karakteristiklerinin değerlendirilmesi için yapılan deneysel çalışma, kompaksiyon deneyleri, serbest basınç deneyleri, tek eksenli şişme-konsolidasyon deneyleri, büzülme deneyleri ve zemin-su karakteristik eğrisini elde etmek için gerekli emme basıncı deneylerinden oluşur.

Çalışmadan elde edilen deneysel bulgular göstermiştir ki bentonit miktarı artarken şişme basıncı artmıştır, kurumada ise numuneler üzerinde çatlaklar oluşmuştur, dolayısıyla strüktür bozukluklarına neden olmuştur. Diğer taraftan ise suya doymun halde hidrolik iletkenlikle serbest basınç mukavemetinde iyileşme gözlemlenmiştir. Farklı karışımlardan dolayı oluşan hidromekanik davranışdaki değişimler emme basıncına bağılı olarak irdelenmiş ve değerlendirilmiştir. Sonuç olarak, katı atık depolama sistemlerinde kullanılması en uygun karışım olarak sıkıştırılmış dağ kumu-15% bentonit karışımının olduğu kanaatine varılmıştır.

Anahtar kelimeler: Sıkıştırılmış kum-karışımları, hidro- mekanik parametreler, katı atık depolama sistemleri.

ACKNOWLEDGEMENTS

I would like to express my appreciation to my supervisor Asst. Prof. Dr. Huriye Bilsel for her guidance during the writing of this thesis. The insight she has given me into the Geotechnical Engineering is wonderful and will be beneficial for my future.

Last but not the least, I am more than thankful to my father, Saied Ghadr, and my family for their support by all possible means during these last two years of my stay in Cyprus.

TABLE OF CONTENTS

ABSTRACT.....	iii
ÖZ	v
ACKNOWLEDGEMENTS	vi
TABLE OF CONTENTS.....	vii
LIST OF TABLES	x
LIST OF FIGURES	xi
LIST OF SYMBOLS/ABBREVIATIONS	xiv
1 INTRODUCTION	1
1.1 Background	1
1.2 Objectives and Scope	2
1.3 Outline of the Thesis	3
2 LITERATURE REVIEW	4
2.1 Background	4
2.2 Bentonites as Backfill and Sealing Material	4
2.3 Structural and Microstructural Units of Expansive Clays.....	7
2.4 Water Reaction in Expansive Clays	9
2.5 Hydration Processes of Compacted Expansive Clays.....	11
2.6 Concept of Suction in Expansive Clays	12
2.7 Swelling Behavior of Expansive Soil.....	14
2.8 Bentonite as a Semi-permeable Membrane.....	16
2.9 Hydro-Mechanical Behavior of Compacted Bentonite and Bentonite- Sand Mixtures	17
2.9.1 Drying-Wetting behavior and Soil-Water Characteristic Curve.....	17

2.9.2	Soil - Water Characteristic Curve	20
2.9.3	Structures of the Soil-Water Characteristics Curves.....	21
2.9.4	Air Entry Value	22
2.9.5	Saturation Residual Degree.....	22
2.9.6	Drying Stages	23
2.9.7	Testing Program.....	24
2.9.8	Swelling Pressure and Swelling Strain of Compacted Bentonite and Bentonite-sand Mixtures	25
2.9.9	A Theoretical Model for the Drying of Initially Saturated Soils	28
2.9.10	Normally Consolidate Specimens.....	28
2.9.11	Overconsolidate Specimens	30
2.10	Hydraulic Conductivity of Expansive Soil.....	31
3	MATERIAL PROPERTIES	32
3.1	Introduction	32
3.2	Basic Properties.....	35
3.2.1	Grain Size Distribution of Sands	36
3.2.2	Aterberg Limit Test.....	39
3.2.3	Natural Water Content	40
4	METHODOLOGY	41
4.1	General	41
4.2	Material preparation	41
4.3	Compaction Methods	41
4.3.1	Dynamic Compaction	42
4.4	Unconfined Compression Test	44
4.5	Ultrasonic Pulse Test.....	44

4.6	Oedometer Tests.....	45
4.6.1	Swelling Pressure and Compressibility parameters.....	45
6.7	Suction Measurement in Compacted Samples	48
4.6	Shrinkage Measurements	51
5	RESULTS AND DISCUSSIONS.....	53
5.1	Unimodal Fits.....	53
5.2	Atterberg limit.....	55
5.3	Dynamic Compaction.....	57
5.4	Unconfined Compressions	58
5.5	One Dimensional Swelling-Consolidation Test	60
5.5.1	One Dimensional Free Swelling	60
5.5.2	Compressibility	62
5.5.3	Saturated Hydraulic Conductivity (Ksat).....	65
5.6	Soil Water Characteristics.....	66
5.7	Estimation of SWCC from the Grain-size Distribution Data.....	72
5.8	Estimation of Unsaturated Hydraulic Conductivity	74
5.9.1	Shrinkage curve equation.....	78
5.9.2	Three-Dimensional shrinkage Test Result.....	82
5.10	Ultrasonic Test.....	83
6	CONCLUSIONS.....	85
	REFERENCES	88

LIST OF TABLES

Table 1: Thickness in Å and for completely hydrated layers for different exchangeable cations.....	10
Table 2: Specific gravity of samples used	35
Table 3 : Grain size distribution.....	39
Table 5 : Natural water content.....	40
Table 8: Unimodal fitting parameters	55
Table 6: Parameters obtained from the fitting of the unimodal equation	55
Table 7: Compaction characteristics	58
Table 8: Unconfined compression test results	59
Table 9: Relationship of consistency and unconfined compressive strength of	60
Table 10: Free-swelling properties	62
Table 11: Consolidation test results	65
Table 12: Saturated hydraulic conductivity values	66
Table 13: Fredlund and Xing (1994) SWCC parameters.....	72
Table 14: Van Genuchten (1980) SWCC parameters	72
Table 15: Estimation parameters for natural and washed sand.....	74
Table 16: Shrinkage parameters calculated by Soil Vision software.....	82
Table 17: Compression wave velocity in different samples	84

LIST OF FIGURES

Figure 1: Description of the montmorillonite structure	8
Figure 2: Microstructure of expansive soils.....	9
Figure 3: Schematic illustrations of double layer water, interlayer water, and “free water” in compacted bentonite	11
Figure 4: Soil-water characteristics curve.....	20
Figure 5: Features of soil-water characteristic curve	22
Figure 6: Drying stage: (a) boundary effect phase, (b) initially transition stage, (c) secondary transmission stage, and (d) residual stage of saturation; after	23
Figure 7: Swelling pressure versus suction of bentonite- sand mixtures.....	27
Figure 8: Conceptual behavior of drying	30
Figure 9: General phase in sand – bentonite mixture.....	33
Figure 10: Specific gravity equipment in laboratory	36
Figure 11: Reduction of hydraulic conductivity of sandy gravel versus percentage of bentonite addition	37
Figure 12: Particle distribution of the sand selected in this study	38
Figure 13: Casagrande apparatus	40
Figure 14: Schematic representation of standard compaction mold and accessories	43
Figure 15: Automatic compaction equipment.....	43
Figure 16: (a) Unconfined compression test apparatus and (b) Failure of the sand - bentonite along the weakest plane	44
Figure 17: Ultrasonic test apparatus.....	45
Figure 18: Schematic cross section of an oedometric cell	47

Figure 19: (a) (b) Samples protruding out of rings when swollen (c) Sample as compacted in the consolidation ring (d) Consolidation test apparatus	48
Figure 20: Schematic figure of the filter paper test set up	49
Figure 21: Different suction measurements	50
Figure 22: Filter paper test set up: (a) Filter paper test samples (b) Styrofoam box	51
Figure 23: (a) Shrinkage test samples (b) Shrinkage diametric measurement (c) Shrinkage axial measurement	52
Figure 24: Grain-size distribution curves for sea and crushed limestone sand with the unimodal equation fits.....	54
Figure 25: Atterberg limits of the sand-bentonite mixtures in comparison with pure bentonite.....	56
Figure 26: Compaction curves	57
Figure 27: Unconfined compression curves.....	59
Figure 28: One dimensional free swelling curves.....	61
Figure 30 : Suction test samples	70
Figure 31: Representation of SWCC fit with Fredlund and Xing model (1994).....	71
Figure 32: Soil water characteristics curves, data fit by Van Genuchten (1980).....	71
Figure 33: Soil-water characteristic curve for sea and crushed limestone sand with estimated curve using Fredlund and Wilson PTF.	74
Figure 34: The estimation of the unsaturated hydraulic conductivity by Van Genuchten (1980) model for pressure (7- 717) kPa.....	76
Figure 35: The estimation of the unsaturated hydraulic conductivity by Van Genuchten (1980) model for pressure (717-2867) kPa.....	76
Figure 36: Demonstration of shrinkage characteristics clayey soil	77
Figure 37: Shrinkage curve of sea sand +15% bentonite mixture	79

Figure 38: Shrinkage curve of sea sand +25% bentonite mixture	80
Figure 39: Shrinkage curve of crushed limestone sand +15% bentonite mixture	80
Figure 40: Shrinkage curve of crushed limestone sand +25% bentonite mixture	81
Figure 41: Volumetric, axial, diametric change curve.....	83
Figure 42: Compression wave velocity in compacted wet soil (m/s)	84

LIST OF SYMBOLS/ABBREVIATIONS

Symbols	Meaning
e_w	: void ratio
v_s	: volume of the soil
v_w	: volume of the water
G_s	: specific gravity of soil
RH	: relative humidity in percent
c_u	: uniformity coefficient
c_c	: coefficient of gradation
PI	: plasticity index
PL	: plastic limit
LL	: liquid limit
q_u	: unconfined compression strength
ϵ_{fail}	: failure strain
E	: elasticity modulus
t_s	: ending time of the primary swell
c_c	: compression index
c_s	: swell index
pc	: pre-consolidation pressure
k_{sat}	: saturated hydraulic conductivity
k_{unst}	: unsaturated hydraulic conductivity
$w(\psi)$: characterizes the gravimetric saturated water content

- w_s : the saturated gravimetric water content
 a : soil parameter linked to the AEV of the soil (ψ_a).
 n : soil parameter relevant to the slope
 m : soil parameter relevant to the residual water content
 e : the natural number 2.7183
 ψ : any soil suction (kPa)
 ψ_r : the residual suction (kPa)
 $c_{(\psi)}$: the correction factor
 y : artificial adaptable of integration indicating the logarithm of suction
 a_{ev} : the air-entry value
 θ : represents the gravimetric water content
 θ_s : the saturated volumetric water content
 θ_r : residual volumetric water content
 a, n, m : constant value
 a_{sh} : the minimum void ratio (e_{min})
 b_{sh} : slope of the line of tangency in drying from saturated conditions
 c_{sh} : inflection of the shrinkage curve
 w : gravimetric water content
 S_r : the degree of saturation
 P_p : percent passing at any particular grain-size
 a_{gr} : fitting parameter corresponding to initial break of equation
 n_{gr} : fitting parameter corresponding to maximum slope of equation
 m_{gr} : fitting parameter corresponding to curvature of equation
 hr_{gr} : residual particle diameter (mm)
 d_m : minimum particle diameter (mm).

Chapter 1

INTRODUCTION

Compacted mixtures of bentonite –sand are usually used in landfill barriers instead of compacted clay, due to low susceptibility to freeze damage and its low shrinkage potential when wetting or drying processes occur (Kraus et al, 1997). However, not all compaction conditions produce a mechanically stable material hence compacted mixtures can collapse and swell upon suction and stress variations.

In the present research work, an experimental program is undertaken including material characterization and hydro-mechanical behavior analyses performed on compacted samples of sand bentonite mixtures with different sand types. The data gained permit a better understanding of the performance of compacted mixtures of bentonite and sand as barrier in waste repositories.

1.1 Background

Bentonite is expansive clay commercially produced from the alteration of volcano ash containing mostly smectite mineral. High swelling capacity and low hydraulic conductivity of bentonite makes it suitable as sealing element and buffer in nuclear waste disposal repositories and as liner in landfills. As the compacted bentonite possesses low hydraulic conductivity, it is anticipated that the leachates from nuclear waste and landfill which flow to groundwater through the compacted bentonite is reduced. Subsequently extreme swelling pressure of bentonite may damage the containers itself; thus a mixture of bentonite with sand is desirable in this case. The

bentonite compressibility, shrinkage, swelling and deformability could be reduced by addition of sand. Moreover, adding sand in bentonite has been found to be beneficial with respect to ease of manufacturing, usage and cost. Research studies have been achieved to consider the characteristics of this mixture and other compacted bentonite-sand mixtures including compaction characteristics, unconfined compressive strength, swelling pressure, consolidation, soil-water characteristics behavior and shrinkage.

Although many research studies have been performed on the hydro-mechanical and thermo-hydro-mechanical characteristics of bentonite-sand mixtures, not many efforts have been made to consider the characteristics of these mixtures as affected by sand gradation. This study focused on the hydro-mechanical performance of sand-bentonite mixture which can potentially be used as sealing element in the nuclear waste disposal facility or landfill liner. This included studies on the material behavior in saturated and unsaturated conditions. Concerning the usage of sand-bentonite mixtures in the hazardous and nuclear waste repositories and landfill facilities, the scope of research covers the effect of bentonite content and compaction characteristics with different bentonite and sand ratios (15%, 25%).

1.2 Objectives and Scope

The overall objective of this research was to explore the hydro-mechanical behavior of compacted sand-bentonite mixtures to be used as buffer and sealing components in greatly toxic and nuclear waste container facilities.

The scope of this research is as follow:

- (i) Effect of the bentonite and sand gradation on Atterberg limits,

- (ii) Influence of the bentonite content and sand gradation on unconfined compressive strength,
- (iii) Behavior of compacted sand-bentonite mixture on swelling – consolidation characteristics,
- (iv) Soil water-characteristics with different bentonite and sand contents,
- (v) Behavior of compacted sand-bentonite mixtures on shrinkage behavior,
- (vi) Ultrasonic wave velocity properties of materials.

1.3 Outline of the Thesis

This thesis consists of six chapters. The first chapter includes the background, scope and objectives of the research. The second chapter gives literature study on the hydro-mechanical behavior of clayey soils and sand-bentonite mixtures. The third chapter includes the physical properties of sand and bentonite used in this research. The fourth chapter presents methods that are used to determine the material characteristics. In Chapter five the experimental results of the compaction, unconfined compression, swelling, one-dimensional compression measurements, total and matric suction measurements, shrinkage characteristics, compression wave velocity measurements of the compacted bentonite-sand mixtures are presented. The sixth chapter concludes the outcomes.

Chapter 2

LITERATURE REVIEW

2.1 Background

The bentonite-sand characterization studies offered in this research have been achieved within a highly defined context: the use of this material as a sealant material for high level radioactive waste disposal facilities, landfills, cut off dams, injection and production activities, petroleum drilling, improvement of soft clay characteristics by thermal stabilization, road snow melting systems ,and regions around buried high-voltage cables. For these purposes, its characteristics have been considered from different points of view and under different conditions that have been investigated throughout the entire research study.

This chapter discusses hydro-mechanical properties of compacted bentonite-sand considering different practices. The discussion is began by description of the structure of expansive soils, hydration procedures, water reactions in expansive soil, swelling mechanisms, concept of suction, and bentonite as a semi-permeable film that are very significant to understand related to the study on the hydro-mechanical behavior of sand-bentonite.

2.2 Bentonites as Backfill and Sealing Material

Theoretically the project of high-level radioactive waste (HLW) containers in deep geological application include the structure of an engineered obstacle around the

waste repositories confined by a buffer or backfill materials (Villar and Lloret, 2008). Wersin et al. (2007) presented that in most of HLW repositories, bentonite has been selected as a buffer materials. Due to low hydraulic conductivity, high sorption behavior, micro porous structure, and swelling capacity bentonite is an exclusive and effective barrier material that protect the container and prevents the motion of radionuclide emission from waste package after the repository failure.

Bentonites are crystalline clay that formed by the devitrification and supplementary chemical modification of vitreous igneous materials, normally volcanic tuffs or ashes (Ross & Hendricks, 1945). Bentonite minerals belong to the smectite group, in which montmorillonite is the most prominent one. Pusch (1979) proposed to use compacted sodium bentonite as sealing materials purposed, since it produces following characteristics:

- i. Very low hydraulic conductivity, reducing the influx and penetration of ground waters, since hydrogeological transport is the main radionuclide transfer mechanism.
- ii. High exchange capacity, therefore bentonite has a high capacity for ion adsorption in the occurrence of radionuclide release.
- iii. Sufficient thermal conductivity which prevents the generation of unwarranted thermal gradients and thermal stress around the host rock.
- iv. Mechanical resistance to endure the weight of the repository.
- v. Mechanical properties of bentonite provide homogeneous environment as a barrier, exhibiting plastic behavior to prevent the formation of cracks, and swelling potential causing the self-sealing of existing voids.

Other important material properties of the barriers are as follows:

- i. Desired compressibility, easy compression processing in handling and transport to the disposal facilities.
- ii. Low shrinkage in response to the drying that will probably occur in the area surrounding the canister, in command to avert the formation of a complex of fissures.
- iii. Not so much swelling pressure, to avoid destruction to the system.
- iv. Appropriate deformability, massive pressure generated by the rock and hydration of the expansive elements of the barriers are absorbed and concentrated by deformation of the barrier itself.
- v. Chemical and physical stabilities that give the high durability to system in relation to disposal conditions such as high temperature, chemical gradient, and vapor presence (Yong et al., 1986).

Bentonite-based materials such as sand-bentonite can be performed by dynamic or static compaction (Ito and Komin, 2008). D'Appolonia (1980), Evans (1991), and Shneider (1994) described that bentonite-based which has been used in cut off dams. Although much information about hydraulic conductivity of sand-bentonite mixture has been published (Evans, 1994; Daniel and Choi, 1999; Filz et al., 2001) data about compressibility and strength has been scarce. Compressibility and strength can be significant, when sand-bentonite mixtures are performed in dams or adjoining constructions (Khoury et al., 1992; Filz et al., 1999). Compressibility and strength also influence the stress-state of the consolidated backfill, which in turn affects hydraulic conductivity (Evans et al., 1995). Scope of the research studies on this field

generally includes the derivation of the properties from laboratory data which consist of modeling in large scale test.

2.3 Structural and Microstructural Units of Expansive Clays

Among of very high plastic clays bentonite is one of prominent, which contains large quantity of monmorillonite (or smectites) and water connection in liquid or vapor form causing expansion, because of mineralogical composition of elementary layers or structural units. Mitchell (1993) presents that the montmorillonite structure is composed of units made of alumina octahedral sheets sandwiched between two silica tetrahedral sheets as shown in Figure 1. The composition of an aluminum atom and six hydroxyls produce the alumina octahedral structure with an octahedral coordination whereas a silicon atom and four oxygen atoms in a tetrahedral coordination prepare the silica tetrahedral.

Crystal and plated particles stacked together to form the elementary layers. Bonding force between these layers in dry condition provide by van der Waals and cation exchange force. These types of bonding are fragile and easily broken when water molecules are inserted between them (Mitchell, 1996).

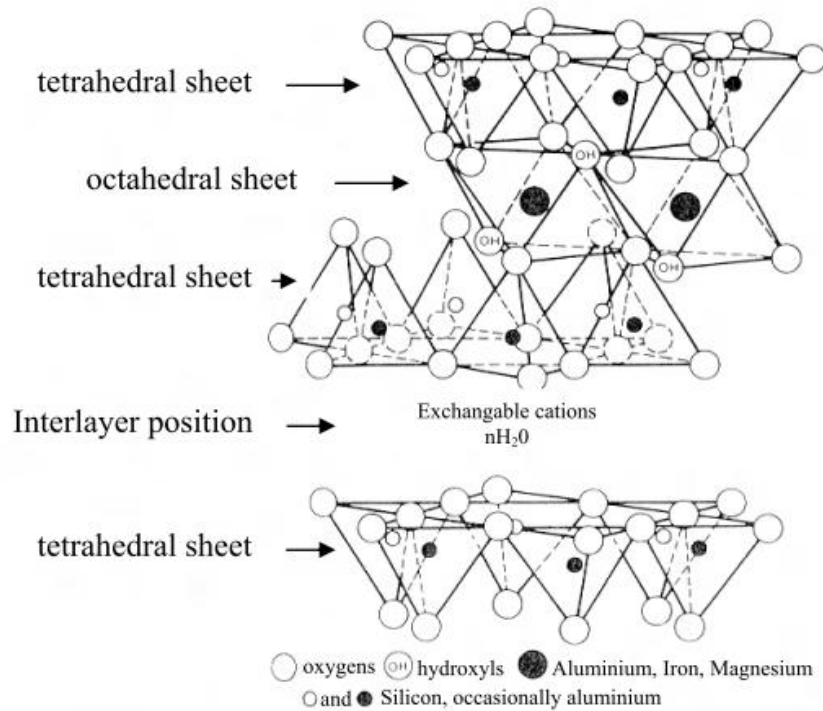


Figure 1: Description of the montmorillonite structure (Mitchell, 1993)

Several to hundred elementary layers make up a clay particle depending on moisture condition (Pusch, 1990). By performing transmission electron microscope (TEM), Tessier et al. (1998) stated that the microstructure of the clay which contains calcium-type montmorillonite and kaolinite minerals, are made up aggregates of particles with 2-4 elementary layers on the average. Number of elementary layer in a particle influences the type of exchangeable cations (Pusch et al., 1990; Mitchell, 1993; Saiyouri et al., 2004). Pusch (1990) presented that each particle produce by 3-5 elementary layer for sodium-type bentonite and calcium-type bentonite procude by 10-20 elementary layers. Saiyouri et al. (2004) reported that number of elementary layers in a particle is affected by compaction operation and the numbers were diverse for calcium and sodium type bentonite for 3000 kpa higher suctions. Also they stated that number of elementary layers in a particle is same for suctions less than 3000 kPa. Bentonite particles stack up and prepare the aggregate. These features are very

significant on the microstructure of bentonite in order to explore the expansive clay behavior (Delage, 2007).

The number of structural units, particles, and aggregates provide different type of pores in expansive clay. Generally compacted expansive soils have two types of pores, macro-pores and micro-pores (Gens and Alonso, 1992; Yong, 1999). The pores within the aggregates (i.e. empty areas between the elementary layers and between the particles) defined as micro-pores or named as inter-aggregate pores. The microstructure of expansive soils is presented in Figure 2.

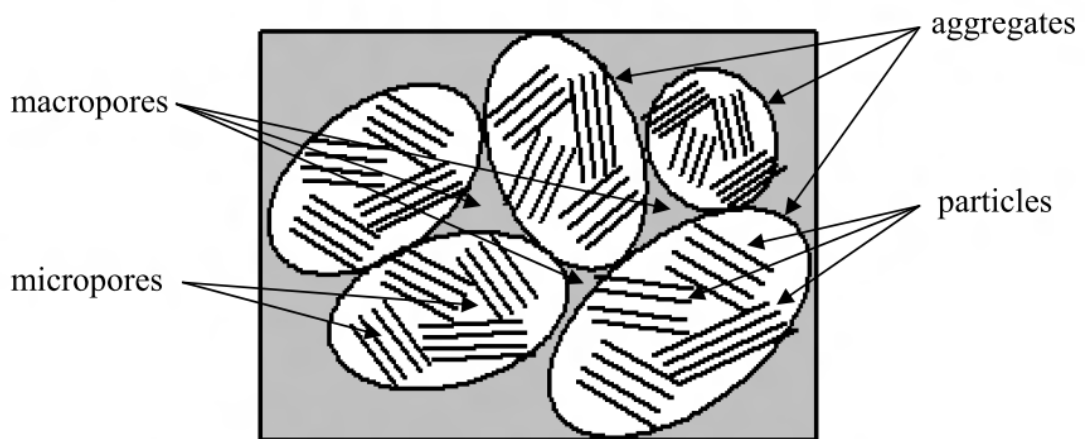


Figure 2: Microstructure of expansive soils (Mitchel, 1993)

2.4 Water Reaction in Expansive Clays

Mitchell (1993) presented the potential mechanisms for water interaction in clay which are exchangeable cations hydration, hydrogen bonding, and attraction by osmosis, attraction by London dispersion forces, and charged surface or dipole attraction. The main mechanism of expansive clays when they are at dry or low water content is hydration of exchangeable cations.

In dry condition, negative charge of clay surface balance with exchangeable cations that are placed on surface of the tetrahedral sheets or layers. Water molecules in hydration process absorbed in between the elementary clay layers to improve the water layers. Different thicknesses of dehydrated montmorillonite crystals and completely hydrate layers are affected by exchangeable cations. Pusch et al. (1990) has stated that the diverse thickness and layers of completely hydrated layers for various exchangeable cations are as presented in Table 1.

As seen in Table 1, three layers of water for Mg and Na bentonite and 2 layers of water molecules for Ca and Na bentonite settled on the clay surface in order to achieve the hydration force. Total water thickness for Mg, Ca, Na, K bentonite types are 9.08, 5.64, 9.74, and 6.15 Å respectively.

Table 1: Thickness in Å and for completely hydrated layers for different exchangeable cations (Pusch et al., 1990)

		0 hydrate	1 st	2 nd	3 rd
Montmorillonite	Mg (001)	9.52	12.52	15.55	18.6
	Ca (001)	9.61	12.5	15.25	-
	Na (001)	9.62	12.65	15.88	19.36
	K (001)	10.08	12.5	16.23	-

Sodium bentonite has specific area of 800 m²/g, which would absorb the water content up to 400 % to fulfill the hydration of exchangeable cations.

Water molecules of mono layers between the elementary layers tend to diffuse toward the surface to equalize ion concentrations, and these phenomena occurs in external surface of particles and crystals (Pusch, 1990; Bradbury and Baeyens, 2002; Pusch and Yong, 2003; Saiyouri et al., 2004). Due to hydration of sodium bentonite particles break up to elementary layers, and diffuse double layers developed (Pusch,

2001). The residual portion of water can be considered as “free water” which exists as inter connected thin film surrounding the mineral grains in bentonite. The content of concentration of dissolved salt in the free water and free water pertain on initial dry unit weight of the specimen (Bradbury and Baeyens, 2002). Water characteristics of compacted bentonite are present in Figure 3.

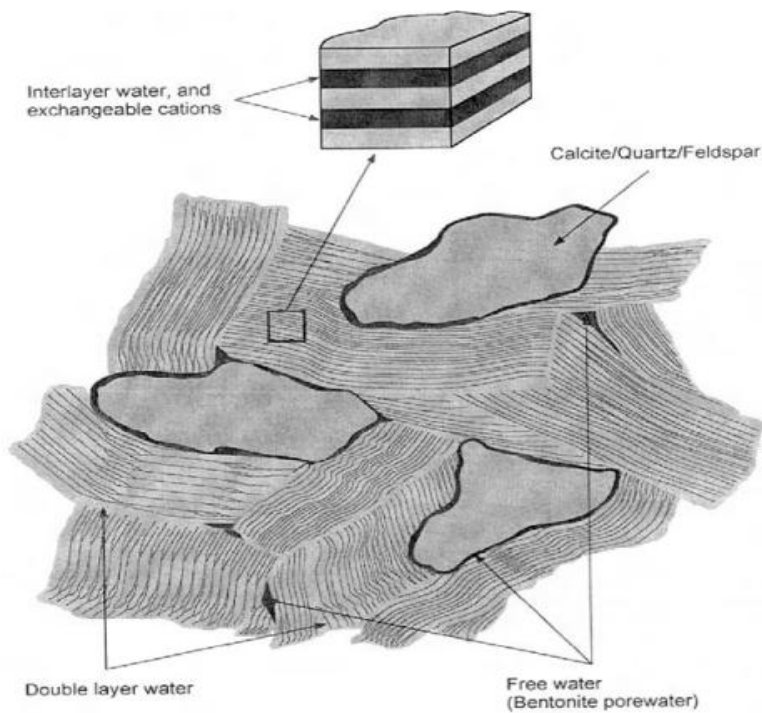


Figure 3: Schematic illustrations of double layer water, interlayer water, and “free water” in compacted bentonite Bradbury and Baeyens, (2002).

2.5 Hydration Processes of Compacted Expansive Clays

There are three boundary conditions which cause dissimilar hydration degree in unsaturated expansive clays. Boundary conditions occur in three conditions, when clays are exposed to water vapor, pressurized water, and non-pressurized liquid water. For clays in contact with water vapor, the water molecules transfer into the open voids and absorbed on exposed mineral surface. The water molecules penetrate

into the elementary sheets that have higher hydration value. The whole penetration procedure of the water molecules is diffusion process.

For the clay exposed to pressurized water, water is constrained into the large channels and transfer rapidly. With water penetration void air displaced and unsaturated matrix compresses. The hydration procedure speed is faster than water exposed to vapor and non-pressurized water. However, when the channels close by growth of clay aggregates, the hydration process become the same as non-pressurized one.

The clay exposed to non-pressurized water, particles absorb the water by capillary force into the open channels, and then mitigate into the finer voids and elementary sheets. Large channels become closed by expanding the clay particles also hydration controlled. In this item, the hydration ratio is slightly higher than the clay exposed to water vapor since the larger channels are filled rapidly.

The hydration mechanism by controlling suction to bentonite was studied by Saiyouri et al. (2004). In that study two type of the bentonite used as FoCa7 and MX80 which are calcium and sodium bentonites. For controlling the suction three methods are performed by applying air pressure in Plexiglas tube for controlling suctions from 1-100 kPa, using membrane cell with a high pressure for applying suctions up to 1000 kPa, and vapor equilibrium system for controlling suction from 3000 to 100000 kPa.

2.6 Concept of Suction in Expansive Clays

Soil suctions consist of two elements, matric suction and osmotic suction (Fredlund and Rahardjo, 1993). The matric suction component has relevance with air-water

interface (or surface tension) giving increase to the capillary phenomenon. Osmotic suction component happens with dissolved solutes in bulk water which is presented as the “free water” in Figure 3. Total suction is sum of the osmotic and matric suction.

Concept of suction mentioned above cannot perform for suction in expansive soils such as montmorillonite due to existence of compressibility of this material due to external pressure and hydration of exchangeable cations on surface. The multifaceted suction improvement in the expansive soil leads to distinguish the relations of soil-water potential and soil suction. Meanwhile the soil suction does not faithfully describe the different devices improved by the sets of thermodynamic powers in the expansive soil. Term of soil-water potential in command to describe the soil suction presented for first time by (Yong, 1999). Yong (1999) declared the mechanisms of soil-water potential consist of, osmotic, matric, pressure potential, gravitational, and pneumatic. The matric potential relating to absorption forces between soil particles and soil-water and pressure potential that is principally because of externally applied pressure which are not used for recounting suction for the non-expansive or soils rigid porous. The matric and osmotic aptitudes are responsible for the water holding capacity into the clay or the pressure potential is equal to zero when no external pressure executed on the expansive clays. However, in conditional condition confining performed on soil volume expansion, so pressure potential is not equals the zero. Therefore, at the saturate condition volume of swelling pressure measurement are constant which have balance in matric and osmotic potentials. Thus, the soil suction of specimen has equal value with swelling pressure. At this condition, swelling pressure of specimen is equal to soil suction. Agus, (2005) described that the capillarity force balance the water potential when

specimen is not full saturation or presence of air in the expansive soil. According to the general theory of suction and soil water potential in expansive soil, it can be resolved that the matric suction of soil comes from the capillary component and hydration forces. Consequently, the total suction is sum of the matric suction which establish by hydration forces and capillary components and osmotic suction from dissolve salt in the soil pore water.

2.7 Swelling Behavior of Expansive Soil

When the clay contact with an atmosphere have high vapor pressure or clay disperse in solvent swelling of expansive clays happen. Laird (2006) stated six difference processes controlling of smectite in aqueous systems, which are double-layer swelling, breakup of quasicrystals (or crystals), co-volume swelling, cation demixing and Brownian swelling. Also he mentioned that double-layer swelling, crystalline swelling and the breakup of clay particles dominantly control the swelling procedure of expansive soil.

From 0 to 4 separate layers of water molecules are inserted between elementary layers inside a smectite clay particle when the crystalline swelling produced. Yong (1999) stated that the layer charge, particle size and properties of adsorbed liquid, and interlayer cations are controlled the crystalline swelling. Furthermore Columbic and van der Waals attraction and innate expulsion balance the crystalline swelling (Laird, 2006).

Because of crystalline swelling volume of smectite may increase two times larger than the initial volume, whereas, the swelling pressure can reach more than 100000kpa as outcome of crystalline is swelling (Madsen and Müller-Vonmoos, 1989). Bucher and

Müller-Vonmoos, (1989) described that the heavily compacted motmorillonite or (smectite), the crystalline swelling has major significance pertaining to use as a repression barrier for the nuclear waste container.

Beyond the crystalline swelling, the double layer swelling has significant effect in swelling mechanism. Overlapping diffuse double layer create the double layer swelling in between the particles and elementary layers (Pusch et al., 1990; Bradbury and Baeyens, 2003; Laird, 2006; Mitchell, 1993; Delage et al., 2006). Sridharan and Jayadeva (1982) declared that mineralogical and chemical properties of soil such as cation specific surface area, dielectric constant, the distance between the elementary layers, valance of the cation, and cation concentration in the bulk water. Efforts have been done to compute the bentonite using diffuse double layer theory or swelling pressure of expansive clay (Bolt, 1956; Van Olpen, 1963; Mitchell, 1993; Tripathy et al., 2004).

Larid (2006) described the microstructure of bentonite from elementary layers by using the transmission electron-microscope (TEM) image. The TEM demonstrates that, first the smectite microstructure was made by specific particles (or crystals) that are flexible and bent. Second, the particles are combined together forming a smectite fabric. Third, the connections between particles are both face-to-face and edge-to-face. These particles interrupt to elementary layers because of hydration. This occurrence was also informed by Pusch (2001) using TEM image for the sodium type bentonite (MX80). In large scale of sodium bentonite incorporation of water molecules occurs between the elementary clay sheets. In calcium type of bentonite, incorporation of water between the layers is low. Saiyouri et al. (2004) declared that swelling mechanism after the crystalline swelling in calcium type of bentonite,

repulsion force between the clay particles and aggregates surface plays significant role.

2.8 Bentonite as a Semi-permeable Membrane

When the concentrated salt solution synthesizes compacted clay, the fluid with or without melted salt will flow in reaction to osmotic gradients. Pure water will flow to moderate with higher salt concentration where soil performs as a flawless semi-permeable crust. The amount to which the clay performs as perfect semi-permeable crust is authorized as osmotic efficiency. Barbour and Fredlund (1989) reported that, pore fluid concentration, interparticle spacing, pore fluid chemistry, and void ratio have strongly effect on osmotic efficiency. As Barbour and Fredlund (1989) have shown, the osmotic efficiency versus interparticle spacing and salt concentration has relationship. The Na^+ soils have higher osmotic efficiency than that of Ca^{2+} soil at the same interparticle spacing and salt concentration.

Schanz and Tripathy (2005) considered the soil-water characteristic curves of clays. According to Schanz and Tripathy (2005), the void ratio against suction for Na^+ clays achieved from experiment was placed above those of the intended from physico-chemical concept. Experimental data points for Ca^{+2} were placed slightly below.

Dixon (2000) stated function of the salinity on bentonite that improvement of swelling pressure in bentonite backfill and buffer materials. It was assert that the swelling pressures are artless in compacted bentonite having preliminary dry density of higher than 0.9 Mg/m by ground water salinity in concentration less than 75g/lit.

2.9 Hydro-Mechanical Behavior of Compacted Bentonite and Bentonite- Sand Mixtures

2.9.1 Drying-Wetting Behavior and Soil-Water Characteristic Curve

The relationship between suction and water content for specimen dried from saturated condition and suction of saturation states the soil-water characteristic curve (SWCC). In condition that water content of soil reductions as suction growth following a drying procedure. Normally the wetting path is started from oven-dried condition which is at 1000000 kPa suction. The total suction at zero water content for a various soil was somewhat below 1000000 kPa (Corney and Coleman, 1961). Fredlund and Rahardjo (1993) also presented that gravimetric water content versus suction affiliation for difference sand and clay soils that at zero water content the suction approaches a value of approximately 980000 kPa. Richards (1965) mentioned to this value which supported by thermodynamic considerations.

The SWCC is affected by type of soil, mineralogy, and texture. The consistency limit of the clay affected the SWCC of clay soil type. Fleureau et al. (2002) prepared a prefect correlation between liquid limit and slope of water content versus suction for wetting path and the liquid limit and slope of void ratio versus suction. The liquid limit of clay joint to suction capacity and stress history to made SWCC (Marinho, 2005).

Specimen of special kind of soil with the same mineralogy and texture can have dissimilar SWCC due to diverse initial water content, stress history, compaction energy, and void ratio. Samples compacted at various water contents outcome in different material of the soil (Lambe, 1960; Gens et al., 1995; Delage and

Graham, 1996). Vanapalli et al. (1999) detected that at different water contents, at optimum, wet of optimum, and dry of optimum with the same compaction energy, clay soil has significantly diverse SWCC. They also reported that specimens tested with difference initial water contents appear to be approximately the same in suction ranging from 20000-1000000 kPa. In this range of suction, soil fabric had no influence on SWCC.

The drying path of specimen from slurry shows the high ability to keep water. They also reported that wetting path of specimen from slurry phase was almost the same as specimen compacted on optimum water content.

The effect of axial compaction stress on drying curve of compacted smectite investigates by (Al Mukhtar et al., 1999). It was presented that the water content against suction curve of specimen having higher axial stress as 10 MPa for relative humidity (RH) range from 100% to 98% was placed under that of specimen having lower axial stress (i.e.,1MPa) . The drying curves of specimens were similar for total suction higher than 2700 kPa or RH less than 98%. Al-Mukhtar et al. (1999) also determined that for RH ranging from (0 to 98%) and RH >98%, suction is controlled by micro-pores; their size distribution are not subjective by the compaction procedure. At RH >98%, suction measurements are more delicate to the test boundary conditions and variant in sample densities.

The swelling properties and water retention of the FoCa7 clay under zero applied stress and controlled suction (Delage et al., 1998). They observed the water content and volume change in reversible responses of suction cycles. Air volume was continued constant, during these changes. Physico-chemical bonds present between

the active clay minerals and water strongly affected the reversibility behavior of saturated microstructural level.

The drying-wetting behavior of a heavily compacted sand-bentonite mixture was considered by Agus (2005). The samples have primary dry density of 2 Mg/m^3 , total suction of 22700 kPa, and water content of 9%. Before drying process specimens fully saturate in two conditions; under seating load of 7 kPa, and constant volume. It was determined that both of the specimens have different drying curves. Agus (2005) stated that general main drying such as the void ratio, water content, and degree of saturation versus suction curves, cannot be defined from the experimental results meanwhile the main drying curve should be found from the specimens primarily in slurry conditions. Agus (2005) also described that the suction does not show any substantial increase in the degree of saturation of the specimen when the as-prepared suction with 22700 kPa is a limiting suction below which further reduction does not occur. As seen in Figure 4, it is also established that the drying and wetting paths do not ever exposed the boundaries (i.e., the drying curve of specimen from saturated condition and the wetting curve of specimen from oven-dried condition) that the drying-wetting curves of the as-prepared specimen used was reversible.

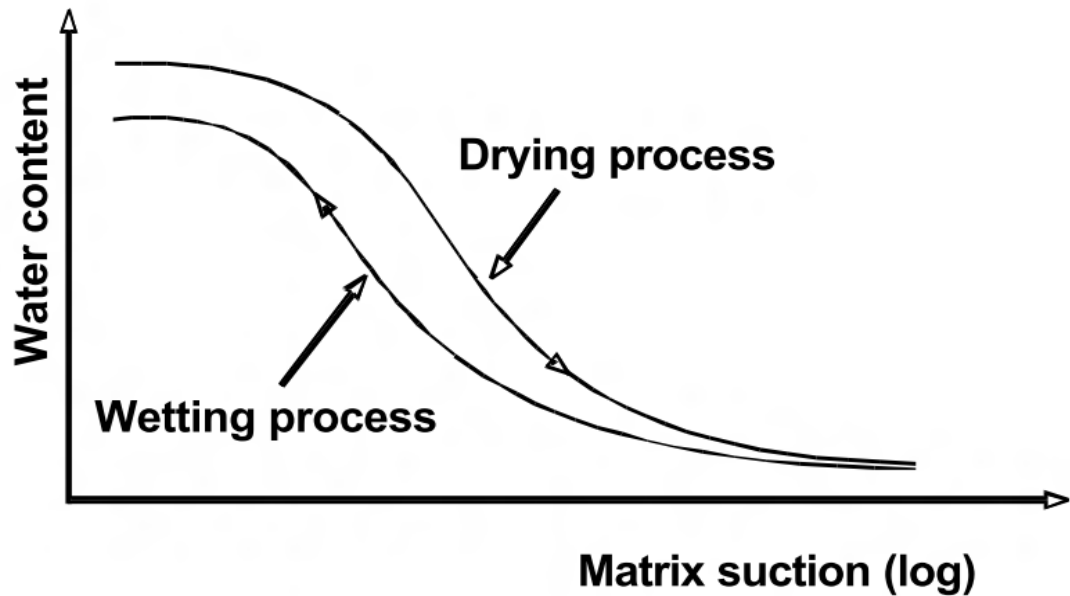


Figure 4: Soil-water characteristics curve (Fredlund, 1964)

2.9.2 Soil - Water Characteristic Curve

The correlation between the suction and water content signifies the soil-water characteristic curve. The result of suction measurement of several specimens having diverse water content performs the different suction characteristic curve. Yahia-Aissa et al. (2000) considered the suction characteristic of an interstratified illite-smectite termed Fourges clay. They obtained that no major difference in the suction against water content relationship was between the powder and compacted samples. The initial condition of specimen such as protector and modified compaction, or loose condition were not effect on suction characteristic curves of bentonite and bentonite–sand mixture (Agus, 2005). The total suction of bentonite-sand mixture is a function of mixture of bentonite content and bentonite water content or concertedly a function of mixture of water content (Agus and Schanz, 2005a). Delage and Cui (2008) declared that the physico-chemical clay-water interactions play a major role in the suction characteristic curve, in compared to the standard hysteretic capillary influences that manage water holding in inactive porous Medias.

Suction measurement methods affect the suction characteristics curve (Agus and Schanz, 2005b), inexactitude of the instrument used (Leong et al., 2007) temperature variation in total suction measurement (Agus and Schanz, 2006a) and mixture of several factors such as inexactitude of the sensors used and temperature variation (Agus and Schanz, 2007). Agus and Schanz (2006b) highlighted that in expansive clay a significance of specimen is reach to the “true” equilibrium state before execution the suction measurement which has relevance to the hydration mechanism in expansive clay (Pusch and Yong, 2003).Furthermore most of clay has a double porosity structure and involves of inter-aggregate pores (Gens and Alonso, 1992; Yong, 1999). The water is sited in the surface of aggregates (macro-pores), when a specimen is integrated with distilled water. The unbalanced total suction between the macro-pores and micro-pores occur after some period of time, an internal redistribution of water is expected to happen.

2.9.3 Structures of the Soil-Water Characteristics Curves

Figure 5 shows a general plot of whole soil water characteristic curve of primary fully saturated soil undertaking a monotonic drying process. Significance features of general curve are the air entry value and residual degree of saturation. Vanapalli (1999) presented that the boundaries between successive stages of the drying procedures.

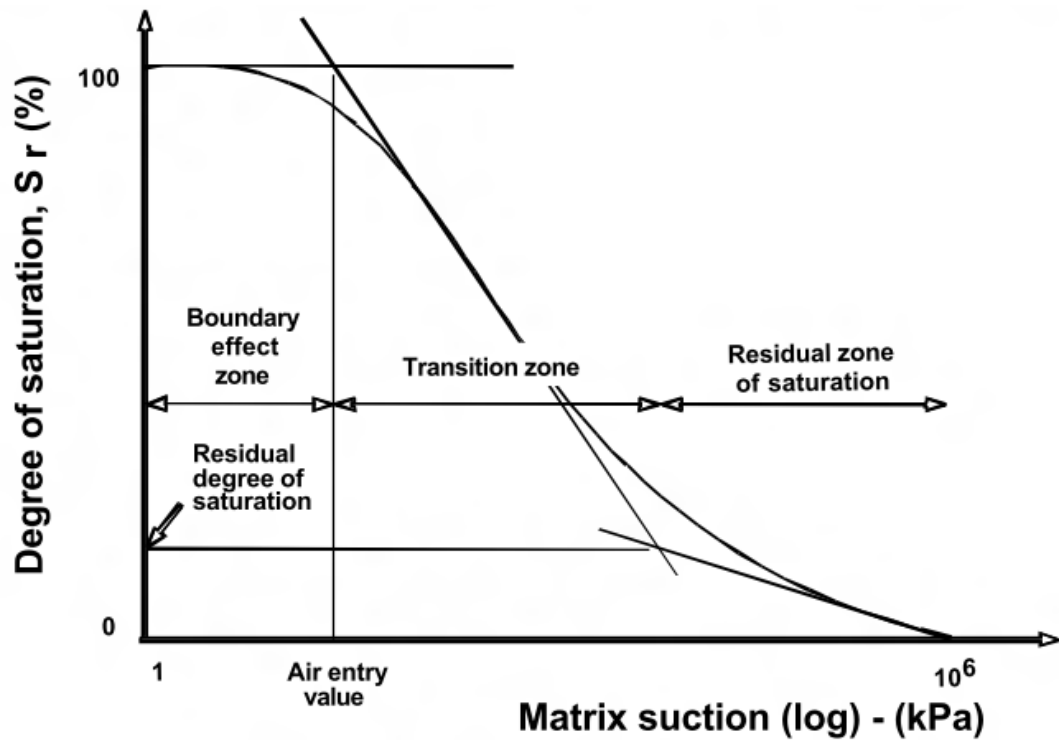


Figure 5: Features of soil-water characteristic curve (Vanpalli, 1999)

2.9.4 Air Entry Value

The suction required to cause air to penetrate in the largest pores of the soil which represent the air entry value. Determination of the intersection of a parallel to line extending the linear slope portion, and the suction axis at a degree of saturation of 100% present the air entry value of simple soil which are shown in the curve Figure 5. The important state to note that, this estimation in entry air degree can be significantly higher than the real suction needed to cause air to penetrate through the largest pores areas.

2.9.5 Saturation Residual Degree

The degree of saturation at which the liquid state becomes halts considered as the residual degree of saturation. Vanapalli et al. (1999) proposed a graphical process for the determination of residual degree of saturation. As shown in Figure 5, the

intersection of a line extending from 10^6 kPa and a line extending the linear portion of the curve is estimated the residual degree of saturation.

2.9.6 Drying Stages

Vanpalli (1996) stated that, during the saturation-drying phase which three definable stages exist as: the boundary influence stage, the residual phase of saturation, and the transmission stage (primary and secondary).

As seen in Figure 6 when soils are in the boundary effect stage, soil particles stay essentially saturated as the suction increases and water content is reduced. Changes in volume are directly related to variation of water content during this stage and the effective stress variable as $(\sigma - u_w)$ which can be used to introduce the soil behavior.

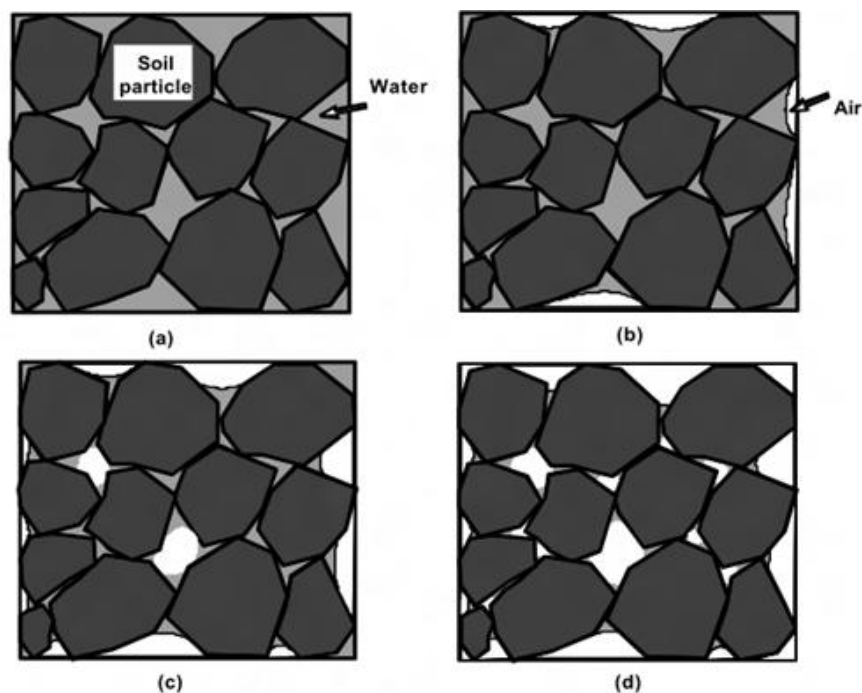


Figure 6: Drying stage: (a) boundary effect phase, (b) initially transition stage, (c) secondary transmission stage, and (d) residual stage of saturation; after (Vanapalli et al, 1996).

With reducing the water content, the tension in the pore water increases and eventually air is penetrate to the soil matrix from the surface. As seen in Figure 6 b, during the primary transition stage, soil suction modest increases due to large reductions in water content.

As gradually more water is substituted by air ,secondary transition stage is started by continual water reducing .Decreasing in volumetric changes are no longer directly correlated to reductions of water contents and source of effective stress becomes invalid (Figure 6 c).

The water is present chiefly in the form of the lenses between contiguous soil particles and air (or gas) is the major pore fluid which identified as the residual degree of saturation stage as presented in Figure 6 d. Relatively small decrease in water content of soil matrix will cause large suction increment.

2.9.7 Testing Program

The soil-water characteristic curves of numerous samples of sand–bentonite compacted at diverse dry unit weight and water contents was calculated and the effect of the dry unit weight and molding water content on the soil water characteristics was assessed .

The testing program was established in three main areas: (1) determination water characteristic curve of compacted specimens of well-graded sand with diverse bentonite contents. (2) An evaluation the sand grading and bentonite content on the soil water characteristic curve, and (3) independency determinate the soil water characteristics of the bentonite and sand.

2.9.8 Swelling Pressure and Swelling Strain of Compacted Bentonite and Bentonite-sand Mixtures

Both swelling strain and swelling pressure are for swelling term in expansive soils. Many researchers who study the expansive soil behavior related to the landfills application had more attention to swelling to swelling potential. Swelling strain also shows the compacted expansive clay ability to swell after a seating load. According to ASTM D4546 and ASTM 1997 the minimum seating load applied in the test is 1 kPa. Mitchell (1993) stated that the swelling strain of clay influenced by initial water content , surcharge pressure , dry density , fabric , and type and amount of clay. Komine and Ogata (2003) declare that the degree of swelling potential besides vertical pressure during the test and initial dry density influenced by the amount of bentonite content in the bentonite-sand mixtures. Swelling pressure is one of the significant issues in compacted expansive clays behavior, which is a advent of swelling potential (Mesri et al., 1994). Thus the swelling pressure developments of expansive soils are similar to the swelling mechanism and it is also performed in the existence of water. The soil at the equilibrium void ratio, the amount of pressure performing on expansive clay at which the soil swells upon wetting signifies the swelling pressure.

When water is added to an expansive soil, the pressure needed to maintain constant volume conditions is swell pressure. This definition has been defined for various test methods. Sridharan et al. (1986) presented the three different methods; namely, swell-load, constant volume test, and swell-under-load. Swelling pressure measurements using oedometer are also designated in ASTM D 4546.

The initial dry unit weight of the samples are controlled the swelling pressure of compacted expansive soils (Sridharan et al., 1986; Komine and Ogata, 2003; Villar and Lloret, 2004; Agus and Schanz, 2005a). In case of sand-bentonite mixture, dry density and bentonite content of mixture affected the swell pressure (Agus and Schanz, 2005a).

Agus and Schanz, (2005a) stated that the degree of swelling pressure of compacted bentonite-sand mixtures determined by using plot of time versus pressure divided by maximum swelling pressure. It was found that the Preliminary total suction of the sample affected the rate of swelling pressure improvement. The outcome of density performs a main role in the low bentonite dry density and heavily compacted bentonite-sand mixture.

The constant volume wetting behavior and swelling pressure of heavily compacted 50/50 bentonite–sand mixture specimen was investigated by Agus (2005). He has presented two different methods, vapor equilibrium technique (VET) for suctions higher than 2000 kPa and axis translation technique for suction less than 2000 kPa. It was established that very small development of swelling pressure happens upon wetting from the as-prepared suction (22700 kPa) to about 2000 kPa suction, in the swell pressure development at constant volume condition as shown in Figure 7. For suctions higher than 2000 kPa there has been very small development in swell pressure due to vapor equilibrium technique (VET). When the specimen is exposed to water vapor, the water molecules penetrate into the macro-pores and immersed on exposed mineral surfaces. The water potential gradient exists between macro-pores and micro-pores are balanced with internal redistribution of water. A postponed ‘true’ equilibrium in the specimen and the ‘true’ equilibrium might be attained after

long test duration, create the insignificant swell pressure development during wetting up to 2000 kPa suction (Agus, 2005).

Agus (2005) also explored swelling pressure enlargement for different bentonite contents and initial conditions of the specimens are as shown in Figure 7. It was presented that the different initial conditions of 50/50 bentonite sand mixture specimens (as-prepared and oven-dried conditions) do not influence the swelling pressure improvement in the specimens. Both specimens demonstrate unimportant swelling pressure improvement at suctions higher than 2000 kPa. Agus (2005) indicated that delayed ‘true’ equilibrium in the specimen with 50% bentonite content is generally related to low hydraulic conductivity of the specimen. The postponed ‘true’ equilibrium also happens to the wet pure bentonite specimen. This is because of the low potential grade of the wet specimen with primary total suction of 18000 kPa which much minor than initial entire suction of oven-dried specimen (Agus, 2005).

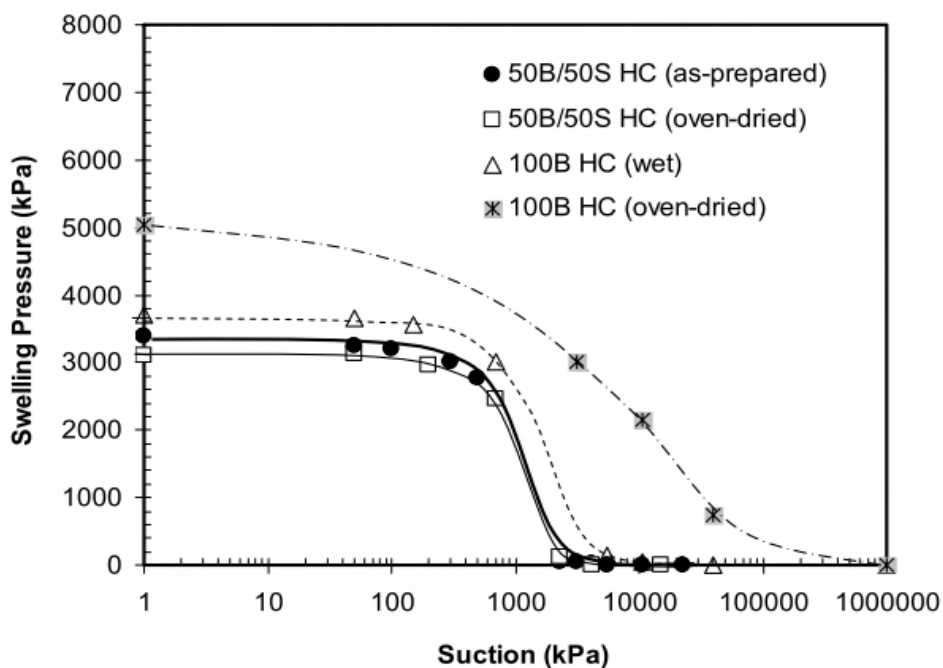


Figure 7: Swelling pressure versus suction of bentonite- sand mixtures (Agus, 2005)

2.9.9 A Theoretical Model for the Drying of Initially Saturated Soils

Toll (1995) proposed that sole water content versus suction relationship exists for initially saturated soils. Normally consolidated expansive soils dry without external stress applied. The virgin drying line (VDL) was defined for the water content versus suction line, and soils on the VDL called normally dried.

Due to re-wetting behavior, soils have also another state beneath the VDL that are called over dried. Over consolidation soils under the fully saturated conditions exist beneath the VDL. Both the over consolidated and oven-dried soils desire to join the VDL if the suction is growth.

2.9.10 Normally Consolidated Specimens

Figure 8 a shows the case of a primarily saturated normally consolidated soil going on to drying. Toll (1995) also calculate the water content of a partly saturated soil on the equal plot as void ratio (i.e. e_w is used as an equivalent void ratio) given in Equation 1.

$$e_w = \frac{v_w}{v_s} \quad (1)$$

Where:

V_s is the volume of the soil

V_w is the volume of the water.

In terms of both e and e_w versus suction shown in Figure 8 (a), soils dried in a semi-logarithmic plot when the soil is fully saturated, e_w is equivalent to e . The line between the A and B points has fully saturated soil condition ($e = e_w$) which pursue

the virgin consolidation line (VCL). At point B the suction spreads air entry volume of the bigger pores medias .The finer pores keep on fully saturated and carry on to diminish in volume change as the suction increases. The overall volume change is smaller than compressed fully saturated soils due to empty pores suction change. At the point B to C in Figure 8 (a) relationships between void ratio and suction have a fewer slopes in compare than VCL line. With further increases in suction, drying path will reach a point elsewhere that the amount of volume reduction becomes negligible. Point C is showing the shrinkage limit in Figure 8 (a). Continual drying process in expansive soil does not produce any further reduction in volume. Continual drying in expansive soil does not offer any further declining in volume.

During drying process beyond point B, the volume of void is greater than the volume of water remaining in the soil. With continue the drying difference between the volume of void s and volume of water increase. The suction e_w relationship becomes sharper than the VCL, as presented in B to D points in Figure 8b. Point D with concerning to a condition where the water in the specimen is present into the fine pores. The slope of the VDL reduces when any growth in suction create a small difference in water content.

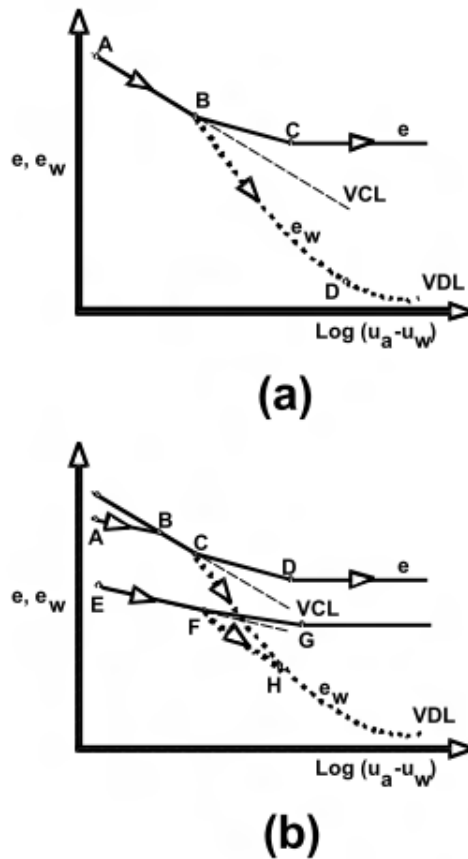


Figure 8: Conceptual behavior of drying

2.9.11 Overconsolidate Specimens

In entirely saturated soils can show smaller void ratios at parallel suctions than normally consolidated samples which are an influence of overconsolidation. Two samples also with various overconsolidation ratios and the equivalent void ratios versus suction relationship represent in Figure 8 (b). The easily overconsolidated soil will primarily pursue the A-B to join VCL thereafter it will pursue the path B-C-D in Figure 8 b which overlaps line A-B-C for normally consolidated soil in Figure 8 (a).

Heavily consolidated expansive soils also attained desaturation at point F beforehand joining to the VCL line. As seen in Figure 8 (b) F to H paths has less steeper than normally consolidated soil before joining to VDL when sample continues to drying with equivalent void ratio e_w .

2.10 Hydraulic Conductivity of Expansive Soil

The saturated hydraulic conductivity (k_{sat}) of sand–bentonite barrier materials is calculated by Darcy's law, and frequently determined under constant-volume conditions by observing the water inlet flow a persistent water pressure by hydrating the sample (Cui et al., 2008). Daniel (1982) stated that the unsaturated hydraulic conductivity (k_{unsat}) can be determined in the laboratory condition by several procedures such as unsteady methods, (i.e. the immediate profile technique), are the most proper for clayey soils declared by (Benson and Gribb, 1997). The k_{unsat} in sand-bentonite buffer materials is often measured from penetration experiments in columns (Cui et al., 2008).

Chapter 3

MATERIAL PROPERTIES

3.1 Introduction

The municipal waste landfill barriers consist of compacted clay covers and liners which should possess hydraulic conductivity less than 1×10^{-9} m/s and mechanical stability during the operation and construction of the landfill. Initial material collection is based on local availability and as an outcome many diverse soil types have been used in landfill liners.

A clayey soil due to low hydraulic conductivity can be used as a buffer material. However, the material with high content of clay or bentonite is likely to swell when wetted, causing instability in barrier systems. Because of high swelling, it also shrinks generating fractures which result in leakage.

Mallins (1996) presented that the sand – bentonite mixture can meet the hydraulic conductivity criteria without suffering from volumetric changes following increment of water content. The sand decreases the shrinkage when bentonite content of mixture is below a limiting amount. The sand particles also have good mechanical support. With respect to bentonite content there are two general phases in sand bentonite mixtures. First, sand particles cannot connect to each other due to high clay content as shown in Figure 9 (a). This material swells when water content increases and shrinks when water content decreases. The second general state when the clay

content is low and sand particles are in contact as depicted in Figure 9 (b), thereby preventing shrinkage and providing mechanical stability. When the mixture is wet, the bentonite particles fill the sand voids producing a very low hydraulic conductivity in compacted buffer liner.

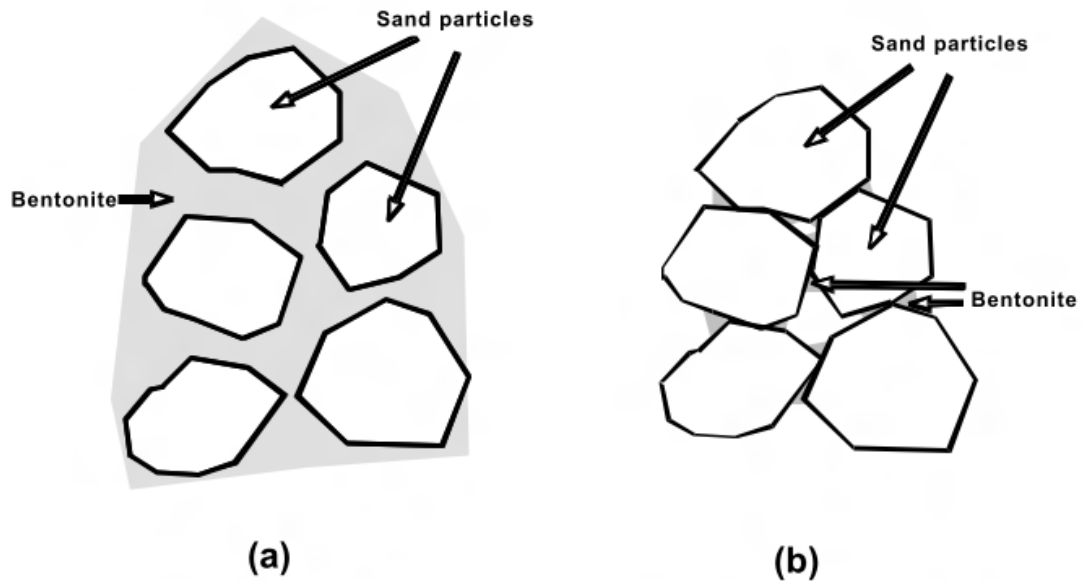


Figure 9: General phase in sand – bentonite mixture

The water content variation after compaction of sand - bentonite liners can either cause swelling or collapse, depending on primary suction and stress conditions. Therefore, laboratory studies of swelling-collapse performance are compulsory to develop a rational attitude to assess the swelling-collapse potential of compacted layers of sand bentonite as landfill barriers.

Bentonite has high expansive behavior, reducing the hydraulic conductivity of mixture to an acceptable value for landfill barriers when used with soils of high hydraulic conductivity.

The usage of bentonite as buffer material can be put into the subsequent categories (Glaeson et al., 1997):

- (1) In geosynthetic clay liner repository, as a low – hydraulic conductivity material.
- (2) As soil stabilizer for compacted buffer material in landfill and waste repository systems.
- (3) As mixture of soil- bentonite or cement -bentonite material in vertical cut off walls that are backfilled.

Most of the bentonites are formed of sodium or calcium as the central molecules. In processing of the bentonite, water adsorbed onto the surface of the clay particle during the mineral formation type of the external cations such as calcium and sodium has important role.

Due to sodium bentonite possessing higher swelling capacity and very low hydraulic conductivity, it is used more extensively than calcium bentonite. Although the calcium bentonite has higher hydraulic conductivity and a smaller swelling capacity to water than sodium bentonite, Galeaso et al. (1997) have suggested that calcium bentonite may be more stable when exposed to chemical constituents than sodium bentonite in permeating fluids.

In this study crushed limestone and sea sand which obtained from Beşparmak Mountains and golden beach in North Cyprus respectively are mixed with Na-bentonite obtained from Karakaya Bentonite Inc., Turkey. This chapter discusses physical, chemical, and mineralogical properties of buffer materials. Several

properties of the material used were obtained from the experiments in this study and the others were gathered from previous studies.

3.2 Physical Properties

The basic properties examined in this study involved the determination of specific gravity, grain-size distribution, and Atterberg limits. The tests were performed based on ASTM standards.

The specific gravity of clay with high plasticity was performed according to ASTM 854-10 (ASTM, 1987) on 7 different types of soils. Soils were poured in distilled water and left for full saturation for not less than 2 hours. The specimens were kept in water for 24 hours in the laboratory, in order to release entrapped air in the specimens. The pycnometers used for this test are shown in Figure 10, in which the saturated specimens were vacuumed by air compressor at equal laboratory conditions. The average specific gravities of specimens are given in Table 2.

Table 2: Specific gravity of samples used

Sample Name	G_s
Sea sand	2.88
Crushed sand	2.74
Sea sand +15 % bentonite	2.70
Sea sand +25 % bentonite	2.64
Crushed sand +15 % bentonite	2.79
Crushed sand +25 % bentonite	2.74
Pure bentonite	2.51



Figure 10: Specific gravity equipment in laboratory

3.2.1 Grain Size Distribution of Sands

A review in case histories and research on mixtures of sand – bentonite shows that a varied range of sand grading have been used based on local availability of materials and the required hydraulic conductivity. However, the research findings reveal that uniform graded sands need a higher amount of bentonite than well graded sands to produce the required hydraulic conductivity. Brandl (1992) presented the variation of coefficient of permeability of river deposits as shown in Figure 11 for compacted sand with different contents of bentonite at maximum Proctor density. They have stated that the lower limit corresponds to a particle size distribution of very well graded materials. Figure 11 provides sufficient guidance leading to the choice of materials.

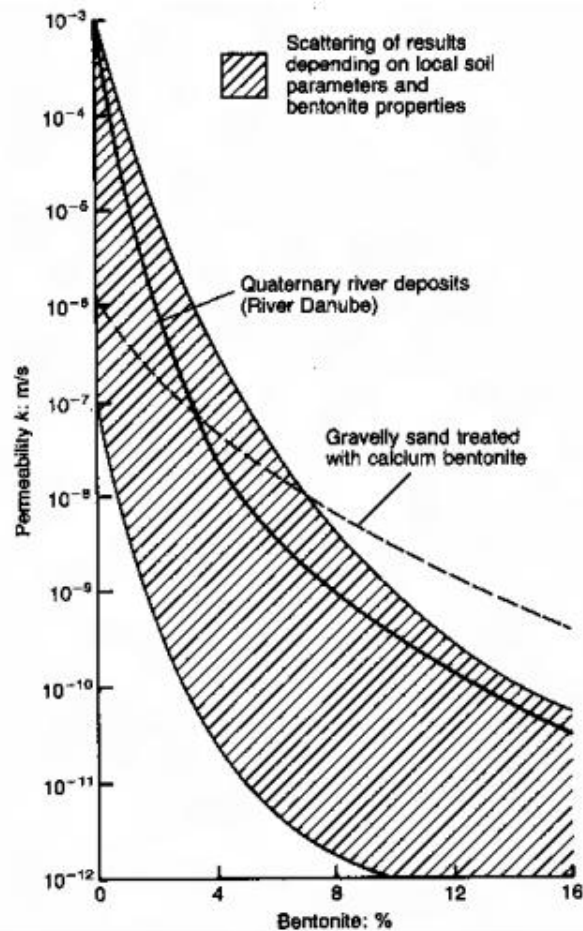


Figure 11: Reduction of hydraulic conductivity of sandy gravel versus percentage of bentonite addition (Brandle, 1992).

Well-graded materials used in the construction of landfill liners will have the following advantages:

- (a) Low volumetric changes potential in contrast to clay or clayey soils.
- (b) The compaction procedure does not require high compaction energy due to reasonably low void ratios.

A current study in U.K. tends to make use of well-graded sand and sodium-activated bentonite. They also propose that the maximum particle size of the sand should not exceed 2 mm (Brandle, 1992).

In this study, the grain size distributions of different kinds of sands were performed by ASTM D421-D422, which showed that the two selected sands corresponded to a well graded sand (crushed limestone sand) and a poorly graded or uniform sand (sea sand). The grain size distribution curves are depicted in Figure 12. Therefore the sea and crushed limestone sand used in this research work possess diverse grain size distribution parameters which are listed in Table 3.

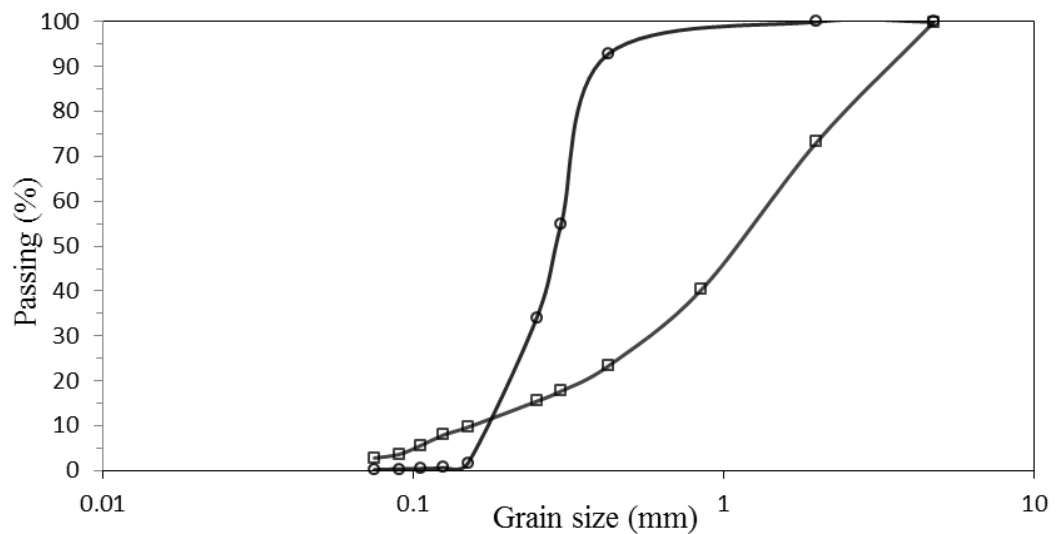


Figure 12: Particle distribution of the sand selected in this study

Table 3 : Grain size distribution

Sample Name	D ₁₀ (mm)	D ₃₀ (mm)	D ₅₀ (mm)	D ₆₀ (mm)	C _u	C _c	Sand Classification
Crushed sand	0.17	0.59	1.14	1.5	8.82	1.37	SW
Sea sand	0.18	0.24	0.29	0.32	1.78	1.00	SP

3.2.2 Aterberg Limits Test

One of the significant characteristics of expansive soils is liquid limit, plastic limit and plasticity index which were obtained by ASTM D4318– 10. The material passing 0.425 mm sieves has been mixed with distilled water and kept in desiccator for 24 hours. The liquid limit test was applied on different soil mixtures using the Casagrande apparatus as shown in Figure 13. Plastic limit of different soil mixtures was determined by rolling the samples on the glass plate and taking the water content of samples which just started to crack when rolled to 3.2 mm diameter, which is considered as the plastic limit. Plasticity index of soils are found by Equation 2. The results are given in Table 4.

$$PI = LL - PL \quad (2)$$

Where:

LL is liquid limit

PL is plastic limit, and

PI plasticity index.



Figure 13: Casagrande apparatus

Table 4: Atterberg limits of the soils used

Sample	Liquid limit (%)	Plastic Limit (%)	Plasticity index (%)
Pure Bentonite	461	41	420
Crushed sand + 15% bentonite	64	21	44
Crushed sand + 25% bentonite	104	24	80
Sea sand +15% bentonite	74	22	52
Sea sand + 25% bentonite	93	24	70

3.2.3 Natural Water Content

The bentonite material due to high expansive behavior when exposed to natural environment can absorb and attract moisture. Natural water content of pure bentonite was obtained both at room temperature and at 50°C, which was the temperature used for drying the bentonite to be used in mixtures, so that higher temperatures would not influence the plasticity index. The natural water contents are presented in Table 5.

Table 4 : Natural water content

Sample	w_n(%)
Bentonite (natural)	12.00
Bentonite (dried at 50°C)	1.88

Chapter 4

METHODOLOGY

4.1 General

Several laboratory test methods have been prepared to characterize the material and to prepare it for the main testing program. They include compaction technique, unconfined compression test, oedometer (swell-consolidation) test, volume change test (shrinkage), and the measurement of soil suction.

4.2 Material Preparation

The bentonite and sand were mixed in semi-arid area and water was added to provide the required water content for compaction. The mixing process was performed for about 7 minutes until the moisture was distributed uniformly. The wet soil mixture was then sealed in several plastic bags and let to mellow for 24 hours before compaction.

4.3 Compaction Methods

Head (1992) stated that the compaction procedure is the process of packing soil particles more closely together by mechanical and rolling means, thus the dry density of soil increased. The soil grains surrounded by a thin water film at low moisture content maintain the grains together. At the same compactive attempt, if the water content is increased the additional water works as a lubricator between the soil particles and allow them to be compacted more effortlessly and simultaneously hence increasing the dry density. When the water content exceeds the optimum amount, dry

density starts to reduce due to excess water pushing the particles apart (Head, 1992). The dry density determined and plotted versus the compaction water content gives the compaction curve. Water content at the maximum dry density is the optimum water content.

In this study, dynamic compaction method has been used.

4.3.1 Dynamic Compaction

Dynamic compaction test methods with ASTM D698-7 covers laboratory compaction methods used to determine the relationship between molding water content and dry unit weight of soils plotted as the compaction curve. The specimens were compacted in a 101.6 mm diameter mold with a 24.5 N rammer weight dropped from a height of 305 mm at a compactive energy of $600 \text{ kN}\cdot\text{m}/\text{m}^3$, the equipment detail are shown in Figure 14. The well-graded and uniform sands mixed with different amounts of bentonite and desired water contents were mellowed for 24 hours in plastic packs, compactions have been performed and each specimen compacted in three layers by 25 blows. The amount of water content determined from three different sections in the mold, the top, middle, and bottom were plotted with respect to the dry densities achieved and optimum water content and maximum dry densities were determined from the compaction curves. The dynamic compaction was applied by the automatic compactor shown in Figure 15.

As an option to the full length stud, a $2\frac{1}{2}'' \times \frac{3}{8}''$ stud may be used. Then as an alternative construction, the collar may be held down with a slotted bracket attached to the collar and a pin in the mold.

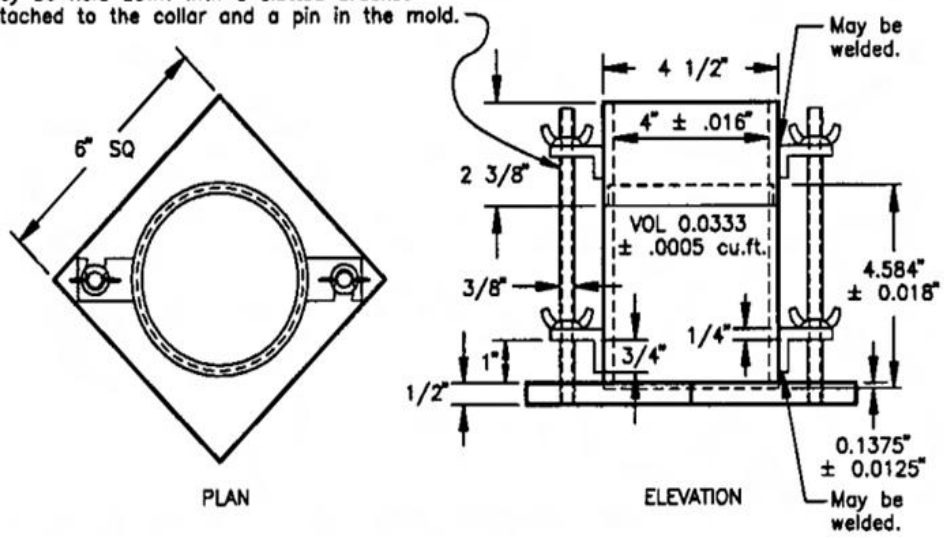


Figure 14: Schematic representation of standard compaction mold and accessories



Figure 15: Automatic compaction equipment

4.4 Unconfined Compression Test

The unconfined compression test is a special type of unconsolidated-undrained test that is commonly used for clay soils based on ASTM D2166-06. In this test, the confining pressure, σ_3 is zero due to no confinement. An axial load is rapidly applied to the specimen to cause failure along the weakest plane. At failure point, the total minor principal stress, σ_3 is zero and the total major principal stress σ_1 is equal to the unconfined compressive strength. The soils were prepared and compacted at optimum water contents, and three specimens were extracted from each compaction mold. Samples had a diameter of 38 mm and height of 76 mm. As shown in Figure 16 the sand bentonite samples were subjected to unconfined compression using the triaxial apparatus.

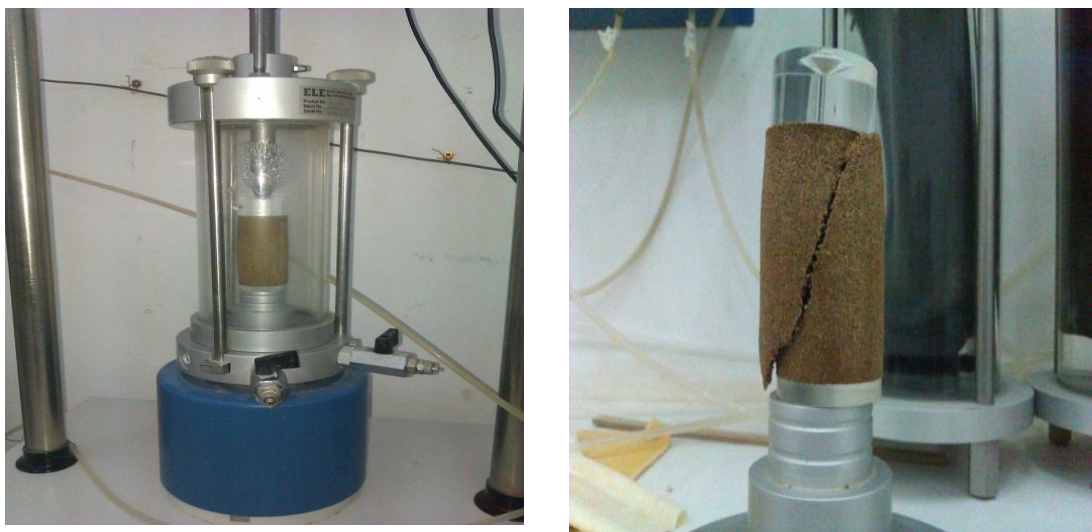


Figure 16: (a) Unconfined compression test apparatus and (b) Failure of the sand-bentonite along the weakest plane

4.5 Ultrasonic Pulse Velocity Test (Pundit)

Ultrasonic pulse velocity test determines the pulse velocity and small strain elastic constants for rocks and soils in accordance with ASTM D2845-95. Soil has high damping compared to other materials, and the test measurement is difficult.

Ultrasonic pulse velocity apparatus receives the compression waves by transducer. The soils tested were either saturated or unsaturated, so the results showed different strain levels in soil. Various samples of sand-bentonite have been used with 15 mm height and 50 mm diameter. Ultrasonic test apparatus was used in this study which transmits the compression wave throughout the samples. Special grease is used for filling the surface pores of samples. The ultrasonic test was applied at optimum water content and at oven dried state.



Figure 17: Ultrasonic pulse velocity test apparatus (Pundit)

4.6 Oedometer Tests

This section describes the methodology applied to determine the swell-compressibility characteristics, swell pressures and saturated hydraulic conductivity values using the oedometer equipment.

4.6.1 Swelling Pressure and Compressibility Parameters

Soils comprising bentonite minerals of expansive or laminar structure are characterized by their high deformability upon hydration, due to the water particles integrated in their structures, thus the distance between the inter-laminate increases. The one-dimensional swell-consolidation test is used to find the equilibrium swelling

pressure applied by a specimen upon complete saturation. For presentation of this test method, the conventional oedometric cells and oedometer frames were exert, in which the surface of the oedometer ring was reduced about 5 mm in order to respond the high pressures probable. The schematic cross section of an oedometric cell is shown in Figure 18. The specimen is confined in a ring preventing deforming laterally, and placed between two porous stones at its lower and upper sides.

According to ASTM D2435 one-dimensional swell-consolidation test has been applied on different samples. This test method is commonly implemented on saturated intact samples of fine grained soils. In this study, these test methods cover techniques for establishing the void ratio versus effective consolidation behavior as well as rate of consolidation and swell pressure of soil under monotonic loading.

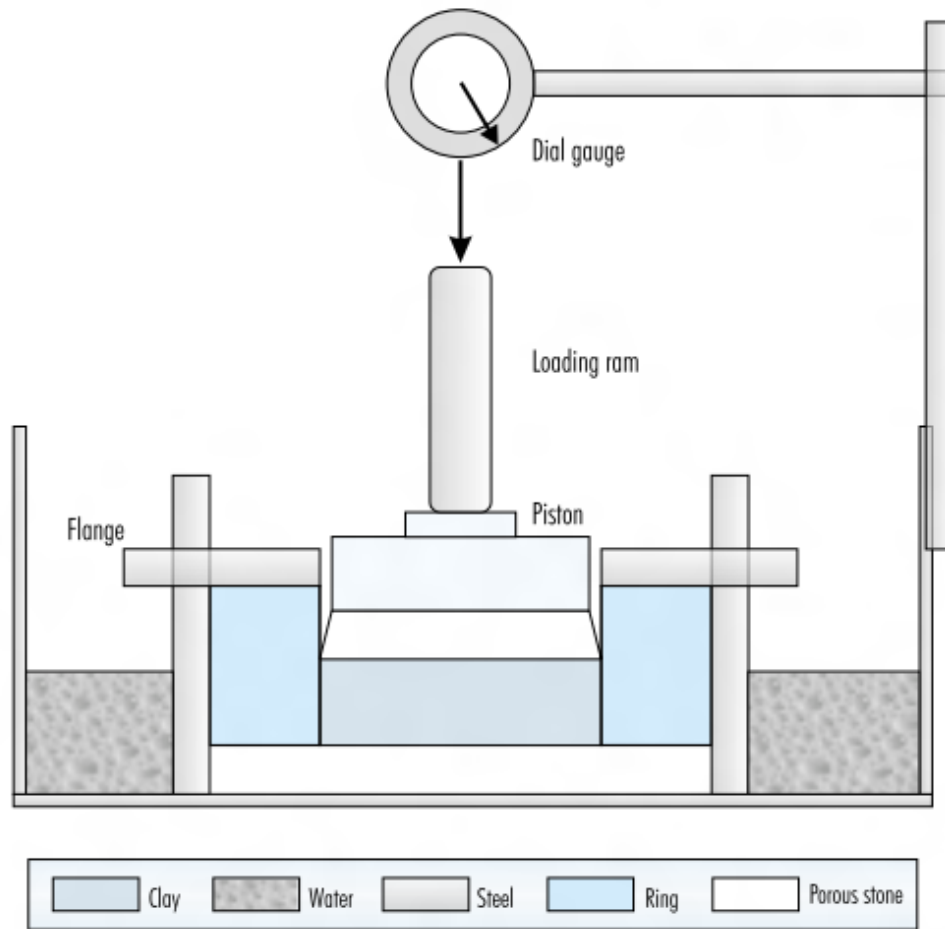


Figure 18: Schematic cross section of an oedometric cell

The soils have been compacted at their optimum water contents and two specimens were extracted from each compaction mold. As shown in Figure 19 (b) the initial height of the ring (19 mm) used was not able to maintain the swelling soil from being damaged due to the high swell potential of samples with higher bentonite inclusion (25%). Thus larger ring height (25 mm) was used for these samples. In order to ensure that, in the event of major swelling, the sample did not protrude out of the ring, the piston was always correctly placed. The sample in the oedometer ring was then placed inside the oedometer cell and the lower porous stone was covered with distilled water, and sample started to saturate from the bottom upwards, letting the air in the pores to emit from the upper part. As the sample saturated under 7 kPa

pressure, the displacements were recorded by the data acquisition system with the help of transducers. Loading stage was started upon completion of one-dimensional swell.

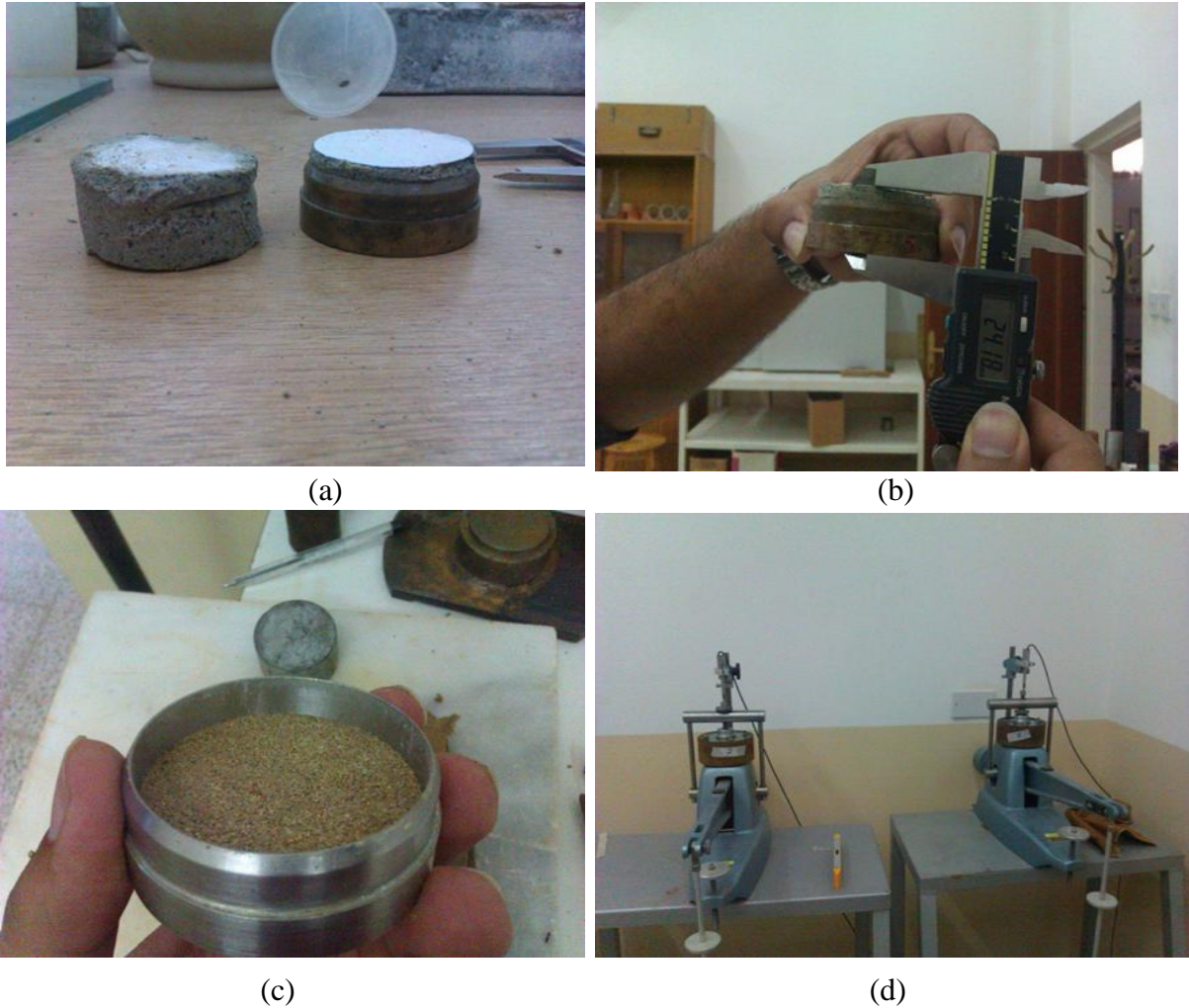


Figure 19: (a) (b) Samples protruding out of rings when swollen (c) Sample as compacted in the consolidation ring (d) Consolidation test apparatus

4.7 Suction Measurement in Compacted Samples

The filter paper method was performed to attain the SWCC of the soils, which is possibly the most widely used technique adopted to test on compacted soil samples. To measure the matric suction of soils, the filter papers were used as sensors, and the method was particularly selected as suctions can be measured in surplus of 1500 kPa. The sand-bentonite mixtures were compacted at maximum dry unit weights at

optimum water contents, and were saturated under 7 kPa surcharges in 50 mm diameter oedometer rings. After attaining full saturation, specimens were exposed to drying at room temperature and their water contents were checked frequently to follow the drying path.

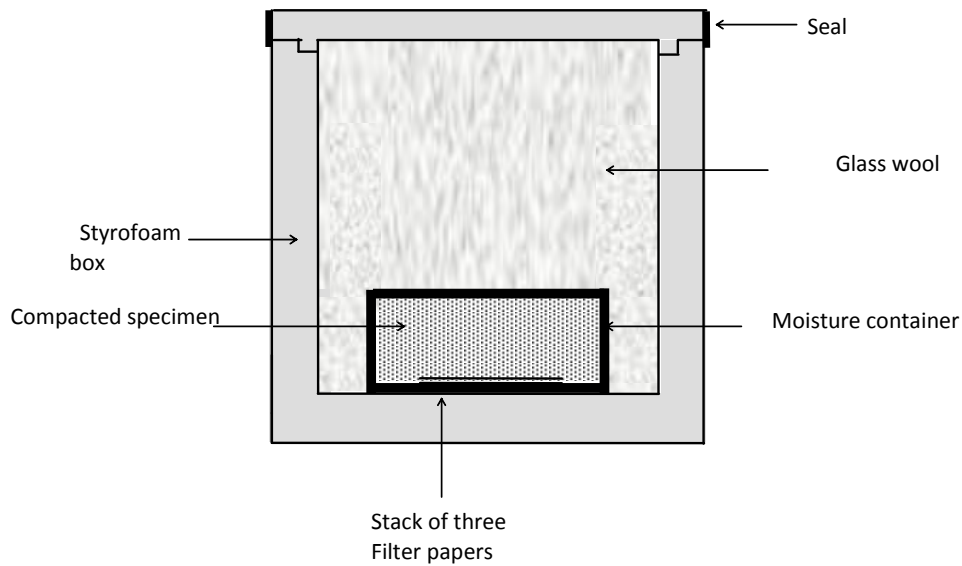


Figure 20: Schematic figure of the filter paper test set up

The compacted sand bentonite mixture samples were placed in intimate contact with 5.5 cm Whatman No. 42 filter paper discs, then sealed tightly in moisture containers and packed in airtight styrofoam boxes. To avert soil pollution, sacrificial filter papers were placed in between filter paper discs and the sand-bentonite samples. The styrofoam box was then filled with glass wool and the cap was closed with two wrappings of sealing tape to ensure good protection. The boxes were reserved at a room temperature ($22^{\circ} \pm 1^{\circ}\text{C}$). As shown in Figure 20, after an equilibration time of 7-10 days, samples and filter papers were taken out for water content determination. The gravimetric water content, w , which is the weight of water in the voids with respect to weight of the dry sample, was calculated. The height and diameter of each

sample was also recorded. The filter paper discs were weighed to a precision of 0.0001g and put to desiccate for 24 hrs at 50° C in the oven. A schematic figure of the filter paper test set up is shown in Figure 22.

For materials compacted statically where the dry unit weight of samples are well below those attained by dynamic compaction, and filter papers achieved lower values of suction than suction probe, when suction probe conforming the calibration line corresponding to primary dry papers, due to the rough surface of samples. In can be seen in Figure 21, for the dynamic compacted samples are in good agreement with the filter paper and the suction probe measurements the reasons for these results are:

- Small variation in temperature happens during the equalization process.
- The air content in the sealed sample is lower in the dynamically compacted samples than in the statically compacted samples due to the densities achieved by each procedure.

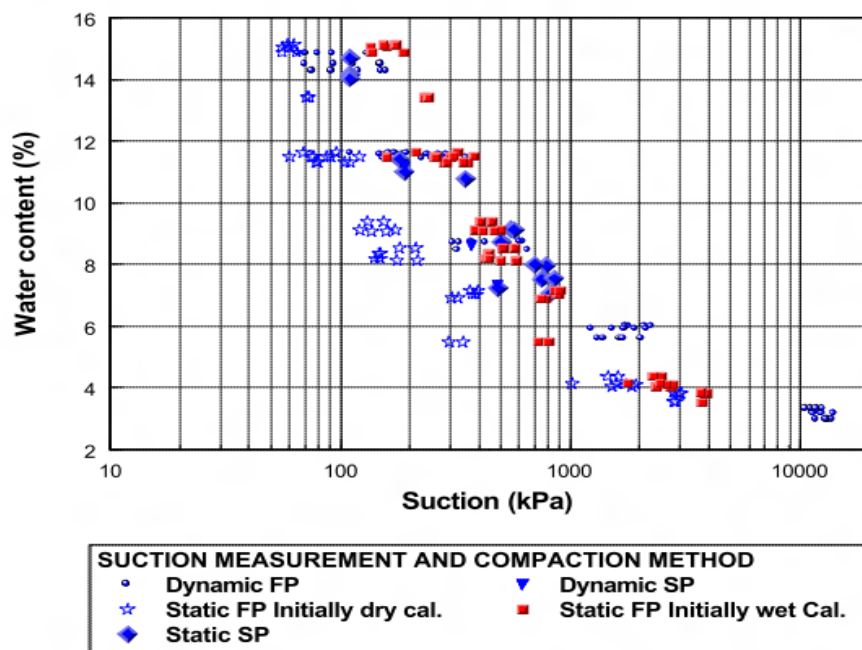


Figure 21: Different suction measurements (Ridely, 1995)

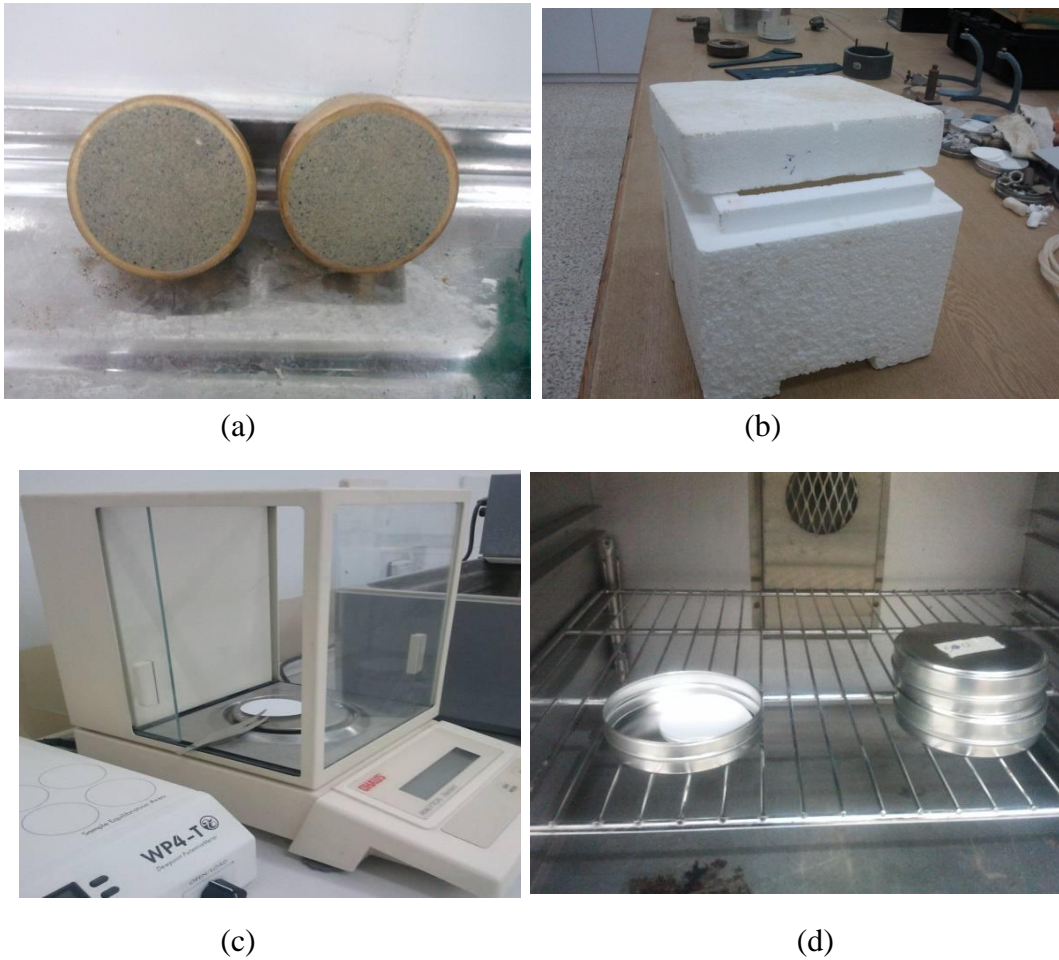


Figure 22: Filter paper test set up: (a) Filter paper test samples (b) Styrofoam box (c) Balance with 0.0001g accuracy (d) Oven for drying filter papers

4.6 Shrinkage Measurements

Sand-bentonite mixtures compacted at their optimum water contents, and saturated in one-dimensional swell-consolidation equipment were drained and allowed to shrink at room temperature (22-25°C). The specimens were weighed and the average diameters and heights were taken every day until they dried to their residual water contents. When no further water content change was observed, the samples were dried completely at 110°C, and the water contents at different stages along the shrinkage path were determined.

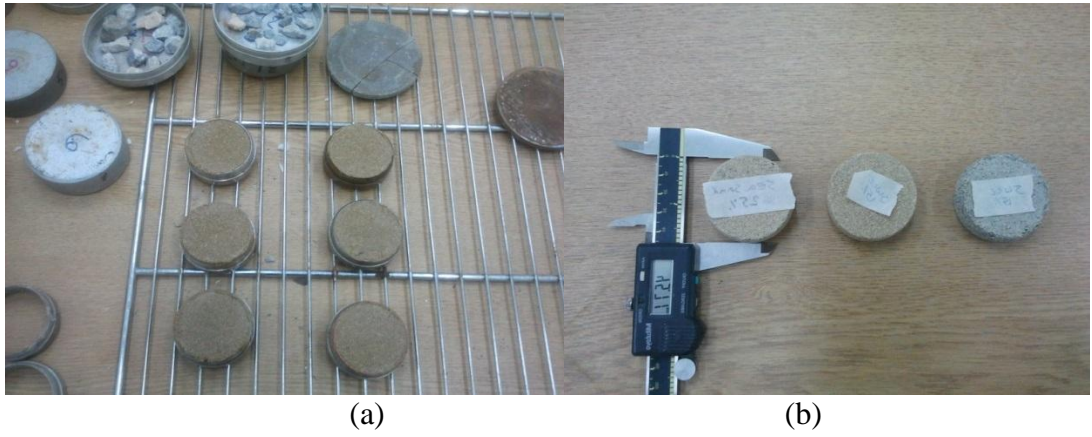


Figure 23: (a) Shrinkage test samples (b) Shrinkage diametric measurement
(c) Shrinkage axial measurement

Chapter 5

RESULTS AND DISCUSSIONS

This section discusses the results of the experimental program which include numerical fitting to the grain size distribution data using unimodal equation, and estimations of soil-water characteristic curve for sands based on this equation, as well as fitting the soil-water characteristic curves of different soil mixtures, and predictions of unsaturated hydraulic conductivity functions.

5.1 Unimodal Fits

Equation 3 presents the unimodal equation, which is advantageous over previous mathematical representations (i.e., log-normal distribution) in the fit of grain-size data of a wide variety of soils. The number of parameters used to represent the grain-size distribution has increased, hence creating complexity, which can be overcome by the availability of curve-fitting software.

Figure 26 shows the laboratory data of the grain-size distribution of two different types of sand and their unimodal fits. Table 8 depicts the particle diameter variables and the coefficients of curvature (C_c) and uniformity (C_u) obtained from the fitting of the unimodal equation to the grain-size distribution data of sea sand and crushed limestone sands. Observing the average size d_{50} of both cases, it can be concluded that the sea sand is finer in average size than the crushed limestone sand.

$$p_d(d) = \frac{1}{\ln \left[\exp(1) + \left(\frac{a_{gr}}{d} \right)^{n_{gr}} \right]^{m_{gr}}} \left[1 - \frac{\ln \left(1 + \frac{h_{rgr}}{d} \right)}{\ln \left(1 + \frac{h_{rgr}}{d_m} \right)} \right] \quad (3)$$

Where,

P_p = percent passing at any particular grain-size, d .

a_{gr} = fitting parameter corresponding to initial break of equation (i.e., representing the large particle size).

n_{gr} = fitting parameter corresponding to maximum slope of equation.

m_{gr} = fitting parameter corresponding to curvature of equation.

h_{rgr} = residual particle diameter (mm).

d_m = minimum particle diameter (mm).

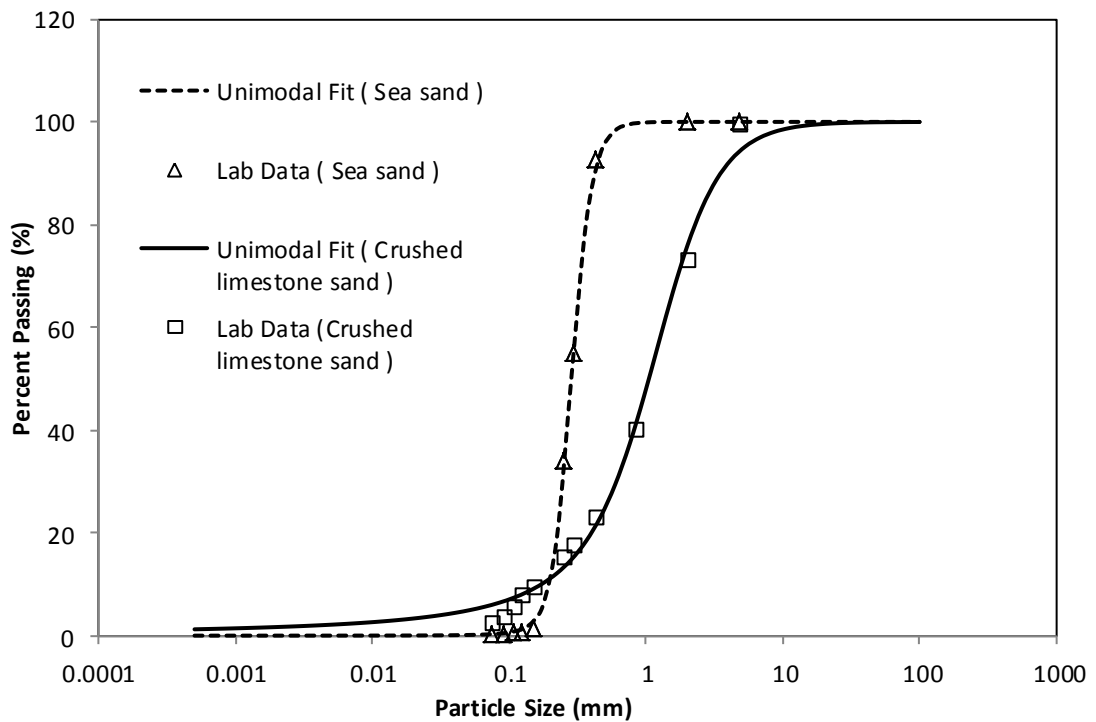


Figure 24: Grain-size distribution curves for sea and crushed limestone sand with the unimodal equation fits.

Table 5: Unimodal fitting parameters

Sample Type	$a_{gr}(mm)$	n_{gr}	m_{gr}	h_{gr}	d_m	R^2
Sea sand	0.27	5.34	3.0	0.001	0.00001	0.9989
Crushed sand	1.48	1.92	1.6	0.001	0.00001	0.9923

Table 9 gives all the grain size distribution parameters of both sands which are the fitting parameters of the unimodal equation. Examining these parameters it can be concluded that while 95% of sea sand particles are smaller than approximately 0.5 mm size, only 25% of the crushed sand is smaller than the same size. Yet while only 5% of sea sand is finer than 0.17 mm size, 10% is finer in the crushed sand. Therefore, even though crushed sand particles are mostly larger in size, there is an appreciable amount of fine particles included.

Table 6: Parameters obtained from the fitting of the unimodal equation

Grain-size analysis results	Sea Sand	Crushed Limestone Sand
d_5	0.1707	0.0521
d_{10}	0.1959	0.1718
d_{16}	0.2149	0.3117
d_{20}	0.2250	0.3990
d_{25}	0.2362	0.5040
d_{30}	0.2464	0.6071
d_{50}	0.2844	1.0501
d_{60}	0.3053	1.3298
d_{75}	0.3449	1.9547
d_{84}	0.3816	2.6413
d_{95}	0.4842	5.2043
C_c	1.015	1.613
C_u	1.559	7.742

5.2 Atterberg limits

In this study it was observed that the influence of grading of the sand is diverse; the Atterberg limits of poorly graded sea sand with higher bentonite contents are greater than those of well-graded sand with the same bentonite content. This may be due to

the maximum particle sizes of the sands. Therefore, plasticity index of sand-bentonite is more affected by the maximum particle size than the grading of sand.

Studying the results presented in Figure 27 it can be concluded that the bentonite content has a significant effect on the Atterberg limits. For pure bentonite the liquid limit is 461% and plastic limit is 41%. However, when mixed with sand, the liquid limit increases from 64% to 104% with an increase in bentonite content from 15% to 25%. The sand–bentonite mixture displays a clayey nature at relatively high water contents. The increasing amount of bentonite mixed with sand increases the liquid and plastic limits, and the plasticity index also increases with bentonite content.

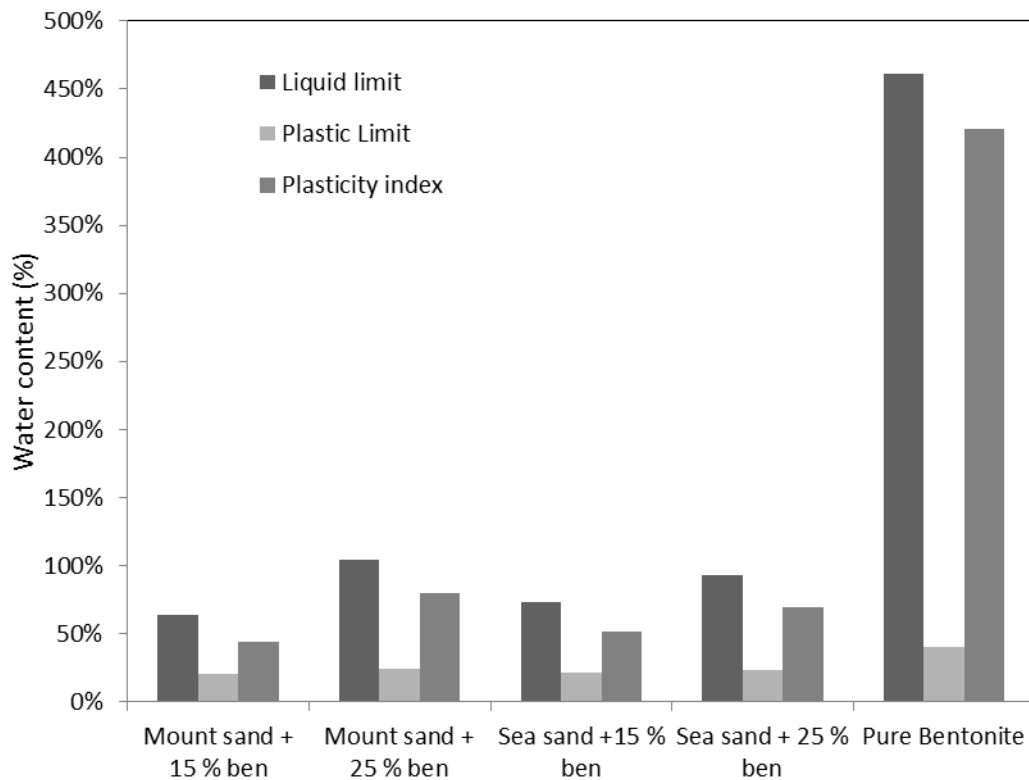


Figure 25: Atterberg limits of the sand-bentonite mixtures in comparison with pure bentonite

5.3 Dynamic Compaction

As shown in Figure 28 and Table 8, increase in bentonite content increases the maximum dry unit weight of sea sand-bentonite mixture, whereas the opposite effect occurs in the well graded crushed limestone sand. In all samples with increasing bentonite content beyond a specific value causes reduction in optimum water content, since water is incompressible and bentonite has high water holding capacity. Alternatively, fine particles of bentonite perform as lubricant between the sand grains and by creating a decent matrix, produces improved compaction and higher dry unit weight. All of the further tests were carried out using these optimum water contents.

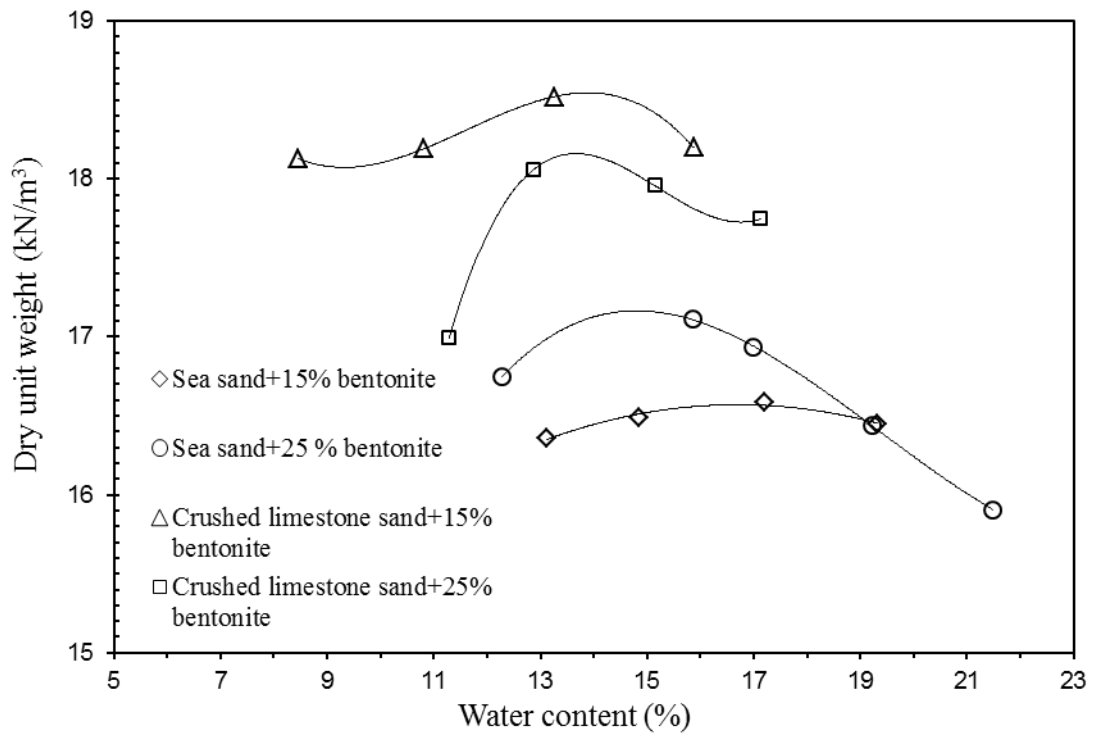


Figure 26: Compaction curves

Table 7: Compaction characteristics

Sample Name	Maximum dry unit weight (kN/m ³)	Optimum water content (%)
Sea sand + 15% bentonite	16.58	17
Sea sand + 25% bentonite	17.17	15
Crushed sand +15% bentonite	18.54	14
Crushed sand +25% bentonite	17.95	12

5.4 Unconfined Compressive Strength

Sand-bentonite samples were prepared with 15% and 25% bentonite contents compacted at optimum water contents and subjected to unconfined compression test. As seen in Table 9 and Figure 27 the samples with well graded sand have higher unconfined compressive strengths than the ones with uniform graded sand. This may be attributed to the ability of the crushed limestone sand to compact easier to a higher density, as well as its crushability under compression, which causes further densification, and thus higher resistance to compression. The modulus of elasticity values of crushed limestone sand included specimens are higher than the sea sand included specimens. The failure strains of crushed limestone sand-bentonite specimens are higher which can be explained with the ability of crushed limestone sand particles, angular in shape, to form better bonding with the bentonite. Therefore, crushed limestone-sand mixtures constitute a stiffer material, which yields at higher strains.

Table 10 gives the relationship between consistency and unconfined compressive strength (Das, 1990). All the sand-bentonite mixtures tested in this research work possess unconfined compressive strengths in the range of 200-400 kN/m², and therefore can be classified as “very stiff” clayey soil except for well graded crushed

limestone sand with 25% bentonite, which has a compressive strength higher than 400 kN/m^2 and classified as “hard” clayey soil.

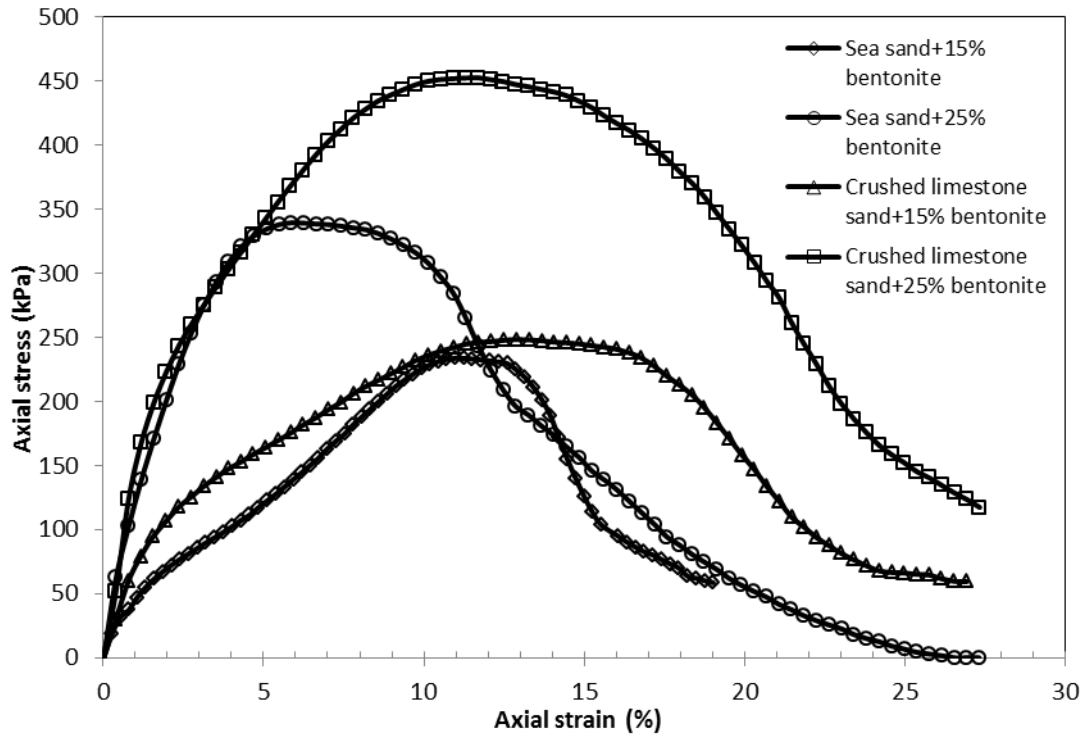


Figure 27: Unconfined compression curves

Table 8: Unconfined compression test results

Soil Type	q_u (kPa)	ϵ_{fail} %
Sea sand +15% bentonite	234	11.0
Sea sand +25% bentonite	343	7.8
Crushed sand + 15% bentonite	249	12.9
Crushed sand + 25% bentonite	453	11.7

Table 9: Relationship of consistency and unconfined compressive strength of clayey soils (Das, 1990)

Consistency	q_u (kN /m²)
Very soft	0-25
Soft	25-50
Medium	50-100
Stiff	100-200
Very stiff	200-400
Hard	>400

5.5 One Dimensional Swell-Consolidation

5.5.1 One Dimensional Free Swelling

Sand-bentonite mixture undergoes through three stages during swelling. First stage is hydration of bentonite particles by adsorbed water in monolayers and second phase of swelling occurs due to repulsion of double-layers which has large volume change supplement with high speed. In the third stage swelling of bentonite particles increase until the swelling pressure of the sand-bentonite equals the vertical pressure.

In this study, free swelling tests were conducted on specimens prepared at optimum water content and maximum dry unit weight. The one dimensional swell versus logarithm of time curves are given in Figure 28. Table 11 gives the swell parameters for four different types of mixtures. In the 15% and 25% bentonite added sea sand samples the primary swell percentages are 28% and 64% respectively. The primary swelling of crushed limestone sand mixtures increased from 40% to 82% for 15% and 25% bentonite additions respectively. The time of completion of primary swell in both types of sand mixtures increased by increasing the bentonite content. Due to very high swell potential of bentonite, after ending the primary swell, the slope of swelling curve continues to increase slightly which gives the rate of secondary swell.

The secondary swell rate increases with the bentonite content, which is more considerable in crushed limestone sand-bentonite mixtures. Both the primary swell values and the secondary swell rates are significantly larger in the crushed limestone sand-bentonite mixtures, therefore it can be concluded that the bentonite has more substantial influence on the well graded sand, which can be attributed to larger pores and surface area in contact with bentonite. Therefore, crushed limestone sand allows bentonite particles to swell easier than in uniform-graded sand mixtures. The swelling properties have important role in the reduction of hydraulic conductivity in landfills, which is the most important parameter in the landfill design.

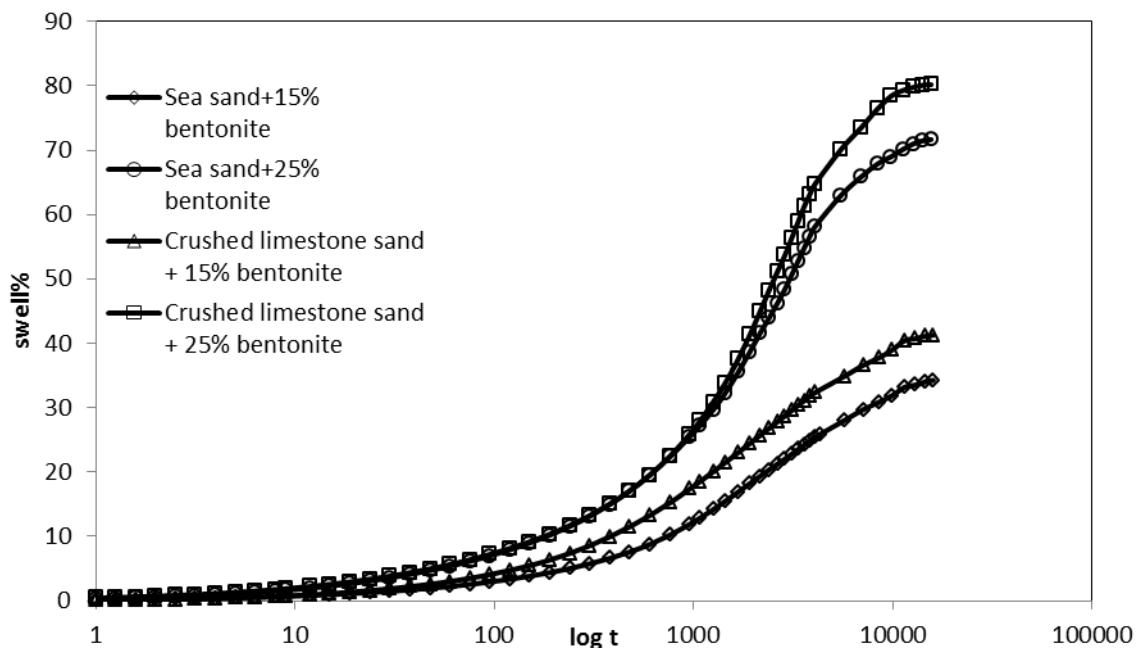


Figure 28: One dimensional free swelling curves

Table 10: Free-swelling properties

Soil Type	Primary Swelling (%)	t_s (min)	Rate of Secondary Swelling
Sea sand + 15% bentonite	28	5000	8.16E-04
Sea sand + 25% bentonite	64	6000	1.39E-03
Crushed sand +15% bentonite	40	7900	2.46E-04
Crushed sand +25% bentonite	82	10000	5.43E-03

5.5.2 Compressibility

The oedometer tests were applied upon completion of full swell under 7 kPa. Experimental results are given as void ratio versus logarithm of effective consolidation pressure in Figure 28. The parameters obtained from these curves, the compression index (C_c), swell index (C_s), swelling pressure (p_s') and preconsolidation pressure (σ_p') are listed in Table 10. Sand-bentonite can exist in two characteristics state: beneath a threshold applied stress bentonite split the sand particles and supports the entire applied stress, whereas beyond the threshold stress matrix of sand and particles support the whole stress that applied in soil (Stewart et al., 2003).

As shown in Figure 29, two slopes of initial part of e - $\log \sigma'$ curves exist which indicates that bentonite of specimens absorb the water and swell. Hence, with the start of loading procedure on the swollen sample at a high void ratio, gradually leaves out the absorbed water till it arrives to the initial void ratio. In this stage major structure of sand bears the stress which is less compressible than bentonite.

Figure 29 also indicates that sand bentonite approximately has a tri-linear characteristic which created three different slopes, with two thresholds. The stresses at which these thresholds occurred are referred to as “threshold stresses” in this

study, and are denoted as p_{t1} and p_{t2} . The average compression indices of the void ratio versus effective consolidation curves, before and after the threshold stresses are shown in Table 12. Studying the parameters given, it can be concluded that the C_{c1} is the slope before the first threshold stress, C_{c2} is between the two thresholds and C_{c3} is the slope of the curve after the second threshold stress. The compression indices between the two threshold stresses are the highest, that is the soil is more compressible right after the first threshold stress, which can be considered similar to pre-consolidation pressure, which once overbeaten, the soil acts like a normally consolidated one, with a steeper compression index. Therefore, the threshold stress, p_{t1} is a measure of cementation initially formed during compaction process. The threshold stress, p_{t2} however develops during the compression of sand and bentonite particles into denser configuration under increasing load, once again forming cementation, which is stronger than the initial case. After this value the compressibility of samples tend to reduce sharply, except in crushed sand-25%bentonite samples which still possess a highly compressible nature after the second threshold. Overall, compressibility of sand-bentonite mixtures increases with increase in swelling and percentage of bentonite content.

Figure 29 shows that the swelling pressure increased with increasing bentonite content. Crushed sand–bentonite mixtures display greater swelling pressures than other mixtures. It is possibly caused by the greater initial dry unit weight and lower water content of crushed sand when the specimens were compacted which is described by El-Sohby and Rabba (1981), where dry unit weight is a significant external factor on swelling pressure. The features of the swelling pressure of the bentonite by constant-volume method, has been established that the swelling velocity increases with the increment of the initial dry unit weight for the same moisture

content (Ye et al., 2007). Mathew and Rao (1997) presented that when the valence of exchangeable cations increases in homoionized smectite clay, the compressibility of the structure is decreased and the pre-consolidation pressure ($\sigma_{p'}$) is increased. This is true for clay alone, however when mixed with sand, the compressibility of the mixture increases up to an optimum bentonite percentage, which has not been targeted in this study. 25% bentonite added sand has higher swell potential, as well as higher compressibility than the 15% bentonite added sand. These properties are even more significant when mixed with crushed sand, which has better compaction characteristics.

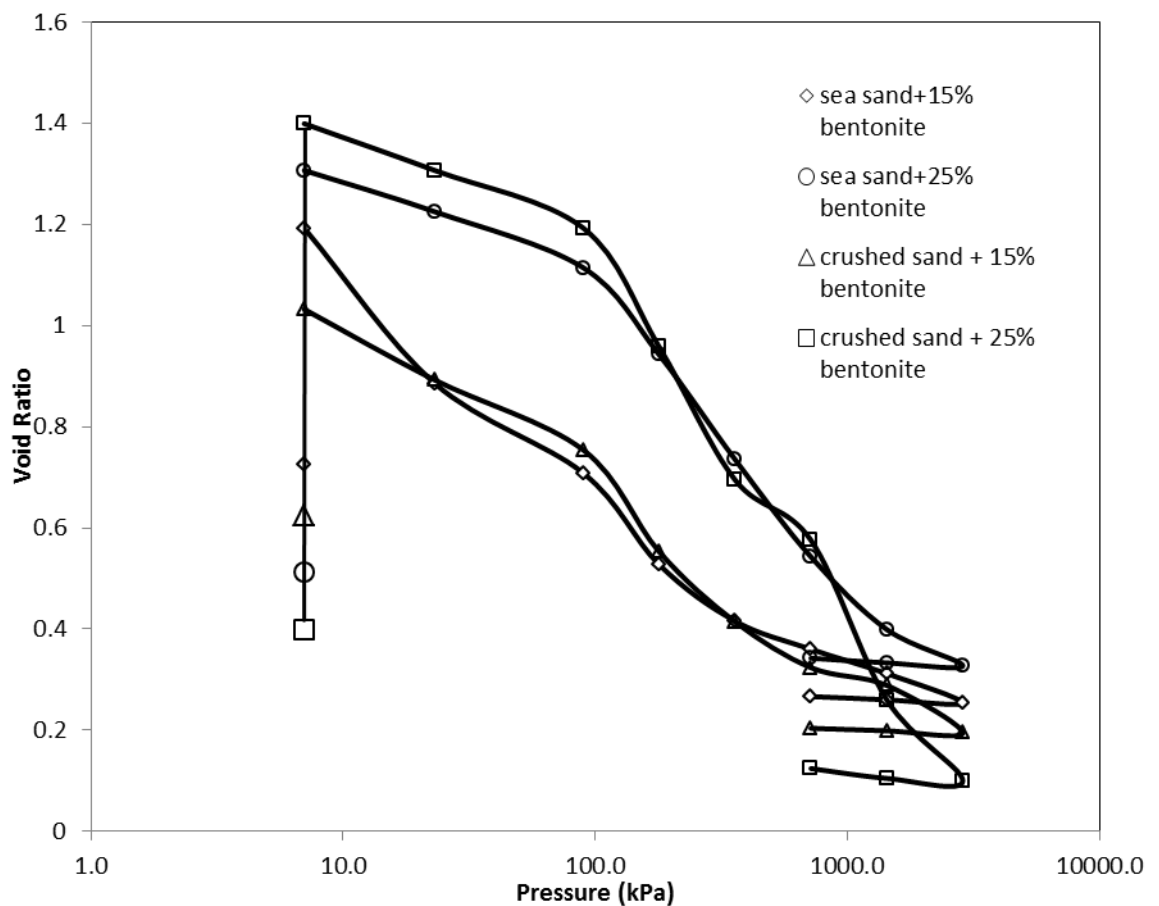


Figure 29: Consolidation curves

Table 11: Consolidation test results

Sample	C_{c1}	p₁₁ (kPa)	C_{c2}	p₁₂ (kPa)	C_{c3}	C_s	Swell pressure (kPa)
Sea sand +15% bentonite	0.44	90	0.606	400	0.20	0.06	80
Sea sand +25% bentonite	0.16	100	0.660	1500	0.23	0.04	850
Crushed sand +15% bentonite	0.24	100	0.520	600	0.20	0.02	131
Crushed sand +25% bentonite	0.26	100	0.780	700	0.60	0.07	1092

p₁₁, p₁₂: threshold stresses

5.5.3 Saturated Hydraulic Conductivity (K_{sat})

The coefficient of consolidation (C_v) gradually reduced with increase in the liquid limit of soil and range of variation of C_v for a given liquid limit is wide (Das, 1990). With increasing bentonite percentage from 15% to 25% coefficient of consolidation increased in both sand types, due to high liquid limit of mixture in 25% bentonite mixture. Well-graded sand has high coefficient of consolidation in comparison of uniform graded sand. Furthermore, coefficient of volume compressibility of sand–bentonite decrease with increase the bentonite content due to high initial void ratio in 15% bentonite content samples.

As seen in Table 13, sand bentonite mixtures have low hydraulic conductivity, because of fine particles of bentonite filling the voids in the sand. Sand –bentonite mixture creates a different type of soil with respect to their permeability, chemical reactions, mechanical behaviors and size distribution. As Kumar and Yong (2002) state that sand-bentonite mixtures due to high specific surface of bentonite particles have low hydraulic conductivity. Bentonite fine particles hold the portion of free water on their double layers and prevent the water from flowing through the sample .

They also conclude that fineness of bentonite and high swell potential have significant role in reduction of hydraulic conductivity. The hydraulic conductivity reduces by increasing bentonite content in both sand bentonite mixtures. The hydraulic conductivity of crushed sand is lower than the sea sand, because of high swelling pressure and less penetrable space between the crushing particles

Table 12: Saturated hydraulic conductivity values

Consolidation Pressure (kPa)	K_{sat} (m/s)			
	Sea sand + 15% bentonite	Sea sand + 25% bentonite	Crushed sand + 15% bentonite	Crushed sand + 25% bentonite
7-717	9.81E-09	1.45E-09	2.85E-09	6.09E-10
717-2867	4.13E-10	1.35E-10	1.71E-10	1.16E-10

5.6 Soil Water Characteristics

The sand-bentonite compacted barriers are often unsaturated in semi-arid areas. Hence, soil suction is the key issue impelling hydraulic properties, strength and volume change. Hydraulic properties consist of hydraulic conductivity, and soil-water characteristic curve (SWCC). An amount of soil water capacity for specified soil suction is SWCC. It explains the relationship between the matric suction, ψ_m ($u_a - u_w$) or the total suction ψ_t (osmotic suction plus matric suction), and gravimetric water content, w . It has a parallel role to consolidation curves in saturated soil mechanics, as it controls the behavior of hydraulic conductivity, volume change and shear strength at various suctions within wetting and drying processes. Thus SWCC can be considered as one of the most significant hydraulic characteristics in unsaturated soils.

In desorption phase, water content of a soil reduces as suction increases following a drying path. Brooks and Corey (1966) described that the air entry value (AEV or ψ_a) is distinguished as the matric suction at the first entry of air into the largest pores in soil sample during a drying process. The water content at the state when liquid phase is discontinues is defined as residual water content, w_r and the soil suction corresponding to this value is the residual soil suction (ψ_r).

In order to achieve the best performance in sand-bentonite containers, it is significant to control the suction characteristics. To describe the highly nonlinear SWCC, various empirical models or equations have been proposed (van Genuchten 1980; Rossi and Nimmo 1994; Fredlund and Xing 1994). The van Genuchten (1980) equation has been widely used by many investigators. Leong and Rahardjo (1997) illustrated that the van Genuchten (1980) and the Fredlund and Xing (1994) equations provide the finest SWCC models for a diversity of soils. For that reason, the van Genuchten (1980) and the Fredlund and Xing (1994) equations were used in this research. The Soil Vision computer software (Soil Vision Systems Ltd. 1999) was used to fit the SWCC using the least-squares algorithm. The Fredlund and Xing (1994) is given in Equation 4:

$$w(\psi) = c(\psi) \frac{w_s}{\left\{ \ln \left[e + \left(\frac{\psi}{a} \right)^n \right] \right\}^m} \quad (4)$$

Where,

$w(\psi)$ characterizes the gravimetric unsaturated water content of sample.

w_s represents the saturated gravimetric water content .

a represents a soil parameter linked to the AEV of the soil (ψ_a).

n represents a soil parameter relevant to the slope at the curvature point (near the air-entry value) on the SWCC.

m is a soil parameter related to the residual water curve .

content portion of the curve.

ψ represents any soil suction (kPa).

ψ_r represents the residual suction (kPa) corresponding to residual water content (w_r).

$c(\psi)$ is corection factor as given in Equation 5.

$$c(\psi) = 1 - \frac{\ln\left(1 + \frac{\psi}{\psi_r}\right)}{\ln\left[1 + \left(\frac{1000000}{\psi_r}\right)\right]} \quad (5)$$

Where ,

ψ represents any soil suction value

ψ_r represents soil suction at residual condition

The van Genuchten (1980) equation is given in Equation 6:

$$w(\psi) = \frac{w_s}{[1 + (\alpha\psi)^n]^m} \quad (6)$$

where,

w_s and ψ have the same definitions as in Equation 3

α represents a soil parameter relevant to the AEV.

n represents a soil parameter relevant to the rate of water removal from the soil, when the AEV has been surpassed.

and m represents a soil parameter relevant to w_r .

The shape of the SWCC described by fitting parameters in both Equation 3 and Equation 4 are attained over best-fitting of test data by the calculated SWCC utilizing a least-squares algorithm (van Genuchten 1980; Fredlund and Xing, 1994).

In this study, drying soil-water characteristic curves were obtained for four different sand–bentonite mixtures using filter paper method. The test results were best fit performing the Fredlund and Xing (1994) and van Genuchten (1980) equations as presented in Figures 31 and 32. The residual water content, air-entry value, and fitting parameters of the SWCCs were obtained by using the SoilVision computer software (SoilVision Systems Ltd.1999) and are listed in Tables 14 and 15.

The air entry values from Fredlund and Xing (1994) model increases with the increasing percentage of bentonite in the sea sand-bentonite mixture which demonstrates the difficulty of air penetrating to largest pores. As seen in Figure 31 and Table 14, due to cracking of the crushed sand 25% bentonite mixture, air entry value decreased from 23.22% to 21.22% with the increase of the bentonite percentage. The cracking was caused as the volume reduction was highest in the crushed sand-25% bentonite sample. In the van Genuchten (1980) model, the air entry value decreases with the increasing bentonite content in sea sand, and increases in crushed sand as shown in Figure 30. As percentage of bentonite increases in the sea sand bentonite mixture, the amount of saturated water content, w_s , increases. The maximum gravimetric water content (w_r), at which the water capacity is near zero and the unsaturated hydraulic conductivity goes to zero, is observed to decrease with reduction in bentonite content. The residual water content obtained by Fredlund Xing

(1994) model increases by increasing bentonite content in sea sand mixtures, whereas it decreases in crushed sand mixture due to fracture. Whereas similar residual water contents were obtained from van Genuchten (1980) model for the four mixtures.



Figure 30 : Suction test samples

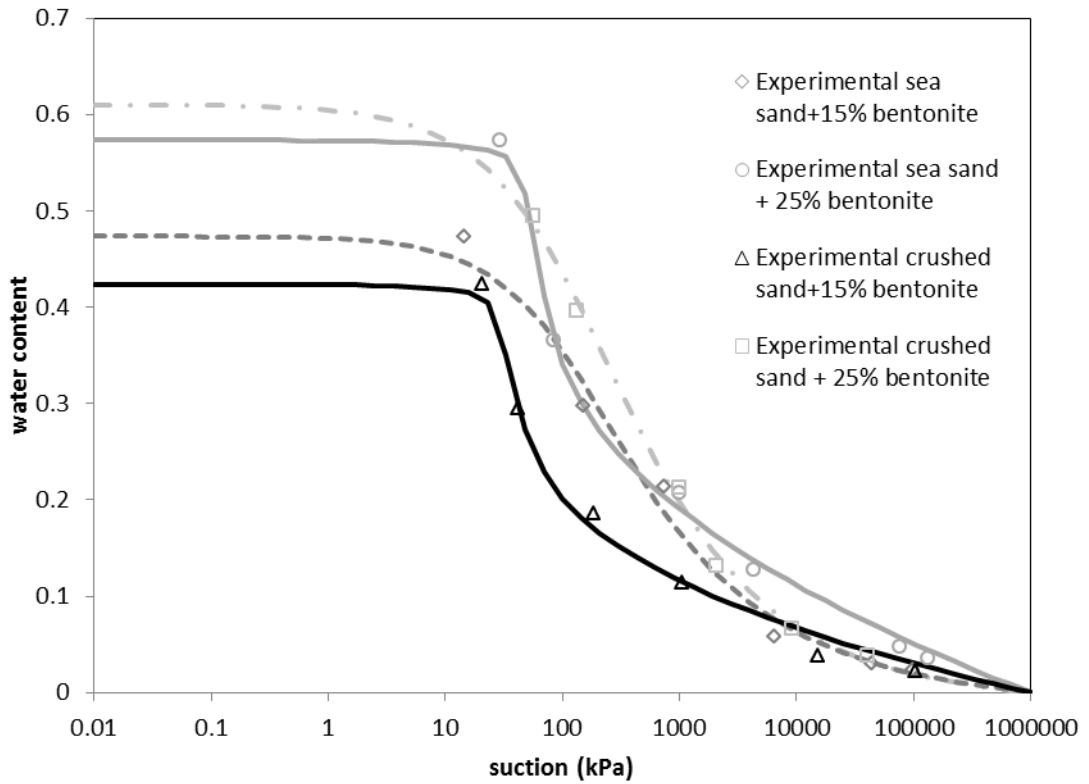


Figure 31: Representation of SWCC fit with Fredlund and Xing model (1994)

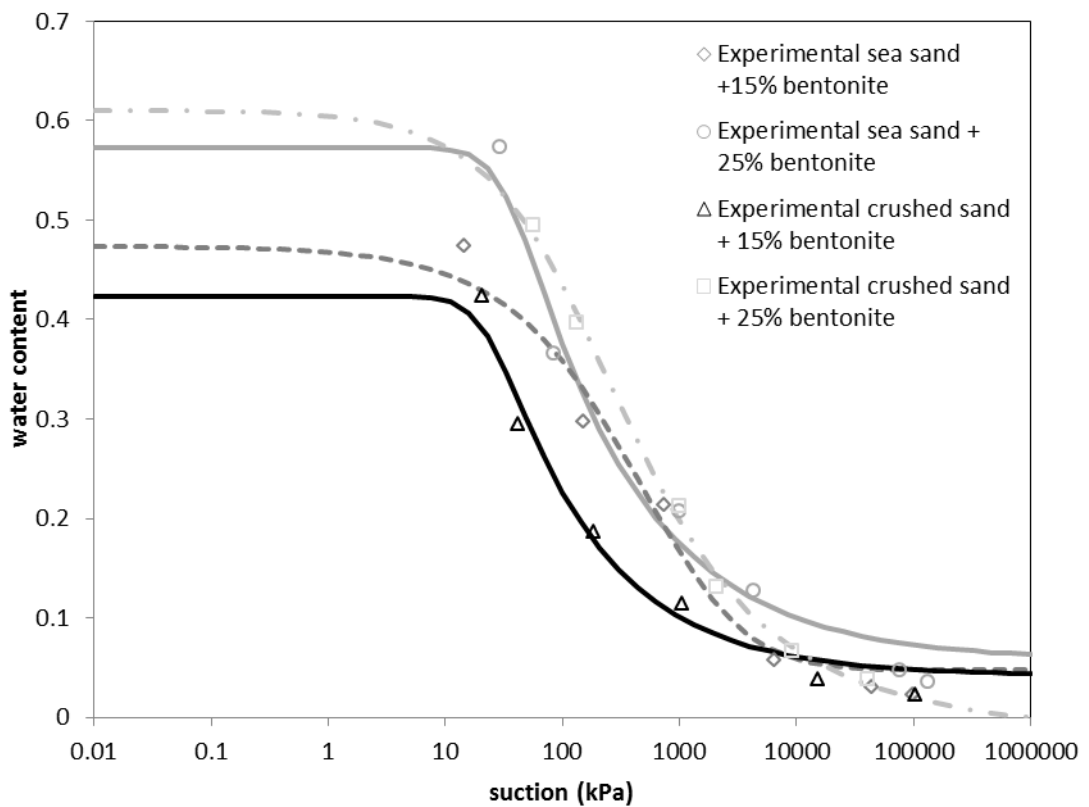


Figure 32: Soil water characteristics curves, data fit by Van Genuchten (1980)

Table 13: Fredlund and Xing (1994) SWCC parameters

Soil Type	a_f	n_f	m_f	h_r	R^2	Fredlund Residual w_R	Fredlund AEV (kPa)
Sea sand +15% bentonite	120.8	0.93	1.18	2320.32	0.985	8%	27.1
Sea sand +25% bentonite	48.29	7.81	0.26	130.704	0.996	23.90%	39.37
Crushed limestone sand +15% bentonite	28.91	6.95	0.30	84.4844	0.992	16%	23.22
Crushed limestone sand +25% bentonite	133.3	0.82	1.46	2507.34	0.996	8.20%	21.22

Table 14: Van Genuchten (1980) SWCC parameters

Soil Type	a_{vg}	n_{vg}	m_{vg}	Genuchten residual w_R	R^2	Genuchten AEV (kPa)
Sea sand +15% bentonite	0.00056	0.6939	2.486	10%	0.9767	33.28
Sea sand +25% bentonite	0.03	3	0.145	10%	0.9751	24.28
Crushed limestone sand +15% bentonite	0.0429	3	0.166	10%	0.976	17.14
Crushed limestone sand +25% bentonite	0.00016	0.6052	4.877	10%	0.993	24.33

5.7 Estimation of SWCC from the Grain-size Distribution Data

The SWCC is related to the pore-size distribution of the soil, and therefore also related to the grain-size distribution. The soil water-characteristic curve has a shape similar to that of the grain-size distribution curve. The mathematical fit of the grain-size distribution can be used to predict the SWCC for a uniform soil, such as pure sand. The Fredlund and Wilson (1997) method for the estimation of the soil water characteristic curve from the grain-size distribution data, is primarily based on the

capillary model as well as a knowledge of the variation of the soil water characteristic curve. The Fredlund and Xing (1994) equation was selected to model the soil water characteristic curve because of its ability to fit the entire range of soil suction. The best fit analysis of Fredlund and Xing (1994) provides three parameters, which can be related to the dominant size on the grain-size plot. Association of m_f and n_f parameters with grain-size can be formed, which in turn can be used to estimate m_{gr} and n_{gr} corresponding to the dominant grain-size.

Fredlund and Wilson (1997) propose to divide the grain-size distribution curve into small divisions of uniform soil particles. A soil-water characteristic curve is estimated for each division, which can then be summed starting with the smallest particle size and continuing until the volume of pore space is equal to that of the entire heterogeneous soil. The result is a theoretically predicted soil water characteristic curve (Fredlund et al, 1997).

Fredlund and Wilson (1997) model is known as a pedo-transfer function (PTF), predicting SWCC using basic soil properties, such as grain-size distribution. As can be observed from Figure 33, and examining the model parameters in Table 16, The air-entry value (AEV), which is the suction at which air starts penetrating the sample during desorption (drying) process, is higher in the sea sand and residual water content also.

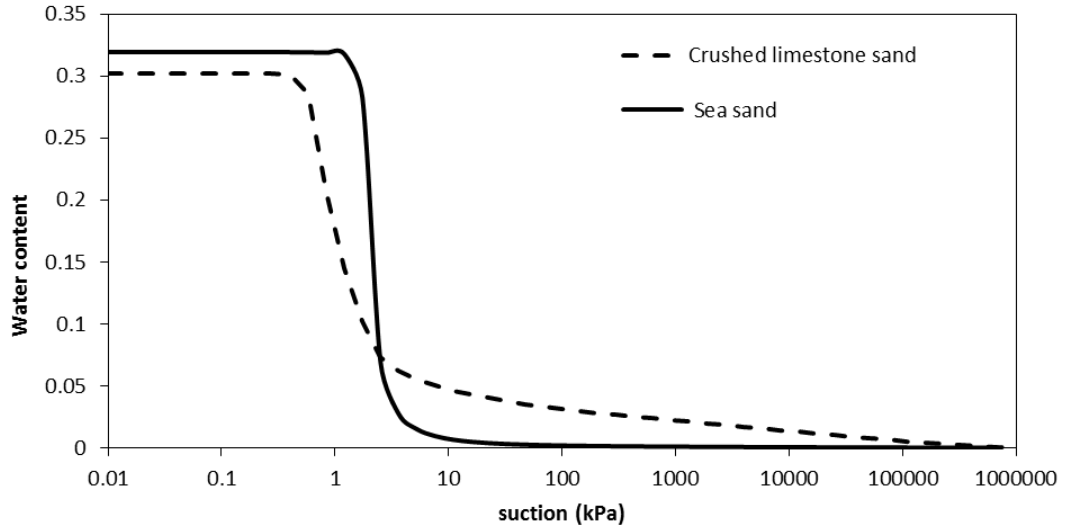


Figure 33: Soil-water characteristic curve for sea and crushed limestone sand with estimated curve using Fredlund and Wilson PTF.

Table 15: Estimation parameters for natural and washed sand

Sample Type	AEV(kPa)
Sea sand	1.6317
Crushed sand	0.533

5.8 Estimation of Unsaturated Hydraulic Conductivity

Unsaturated hydraulic conductivity is not a constant value but a function of soil suction. Numerous research studies have presented that the soil-water characteristics of soils and their unsaturated properties are related (Fredlund et al., 1994). Estimation models for the hydraulic conductivity have recently become important, due to their simplicity and easiness of usage. Hence, it is significant to obtain the SWCC and the hydraulic conductivity function which constitute the hydraulic properties of unsaturated soils in order to study the behavior of unsaturated soil (Ng and Pang, 2000).

Van Genuchten established closed-form equation for the relative hydraulic conductivity function ($k_r = k_\psi / k_s$). Mualem (1986) revised the van Genuchten equation

into the statistical relative hydraulic conductivity model which is described by Equation 7.

$$k_r = \frac{\{1 - (\alpha\psi)^{n-1}[1 + (\alpha\psi)^n]^{-m}\}^2}{[1 + (\alpha\psi)^n]^{\frac{m}{2}}} \quad (7)$$

Where:

ψ represents any soil suction value ,and (kPa)

a,n,m constant value

The estimation and prediction of unsaturated hydraulic conductivity versus soil suction curves from van Genuchten (1980) model with different saturated hydraulic conductivity and pressure are presented in Figure 31 and Figure 32. In low suction values, the sea and crushed limestone sand mixtures with 15% bentonite represent the high permeability in both loading pressures versus the mixtures with 25% bentonite which have low hydraulic conductivity value closer during the desiccation. Sand bentonite mixtures have low hydraulic conductivity in high pressure, due to compressed the sand and bentonite particles with together and decrease the void ratio in samples. The unsaturated hydraulic conductivity of all sand bentonite samples in high suction content is almost zero.

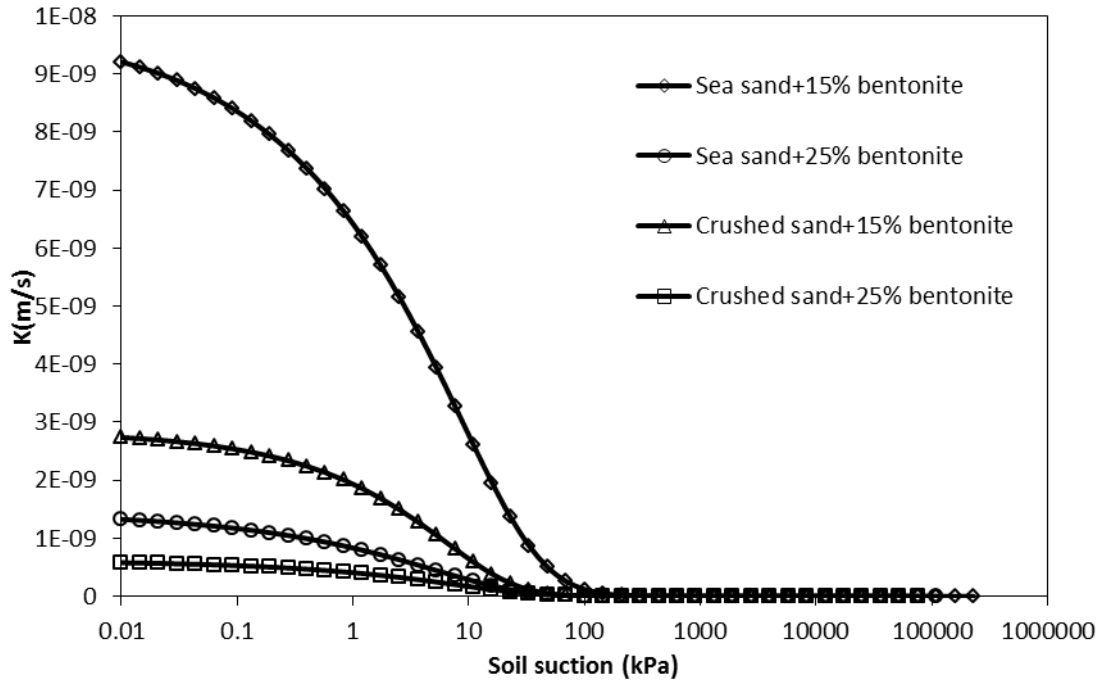


Figure 34: The estimation of the unsaturated hydraulic conductivity by van Genuchten (1980) model for pressure (7-717) kPa

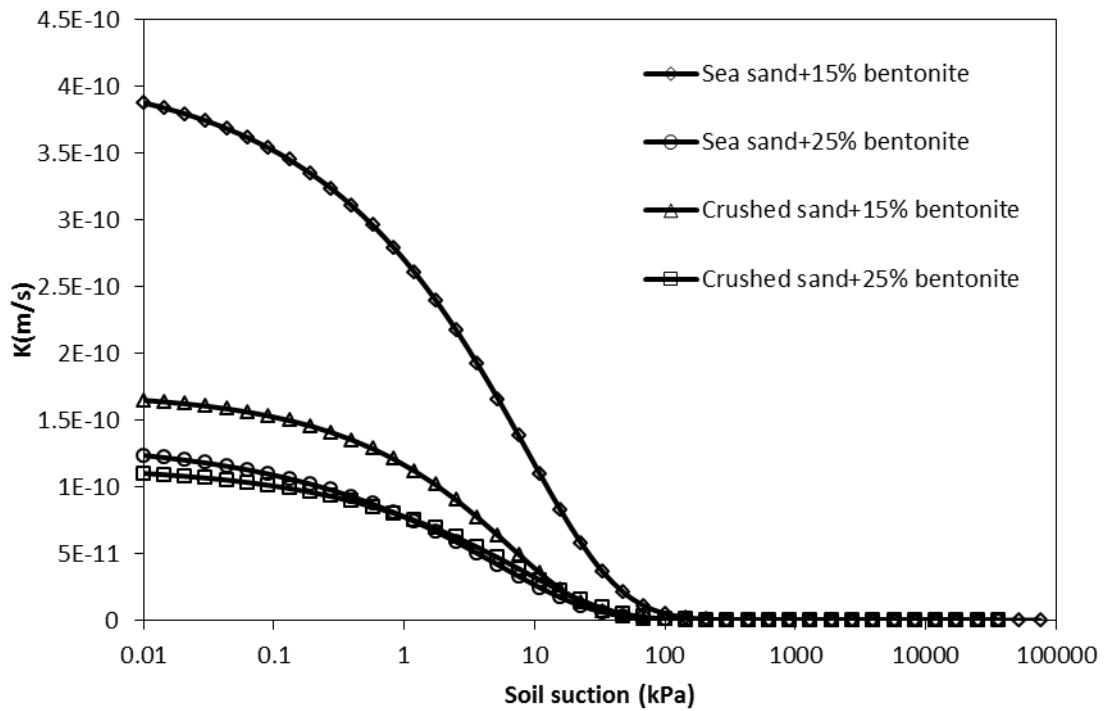


Figure 35: The estimation of the unsaturated hydraulic conductivity by van Genuchten (1980) model for pressure (717-2867) kPa

5.9 Shrinkage Test

Shrinkage limit is the water content at the minimum volume which a soil can attain on the drying path. Shrinkage curve is obtained from an initial high water content condition to entirely dry condition. The shrinkage curves have a significant role in the explanation of SWCC results. Figure 36 shows the shrinkage curve of a drying clayey soil from fully saturated condition. The point at which the shrinkage curve deviates from the saturation line is approximately equal to the plastic limit of the soil. Accordingly, there is an estimated correlation between the air entry value and the plastic limit of a soil. Over additional drying, another point is stretched where the soil dries lacking further change in overall volume. This can be mentioned as the factual “shrinkage limit” of the soil and this gravimetric water content correlates to residual soil situations.

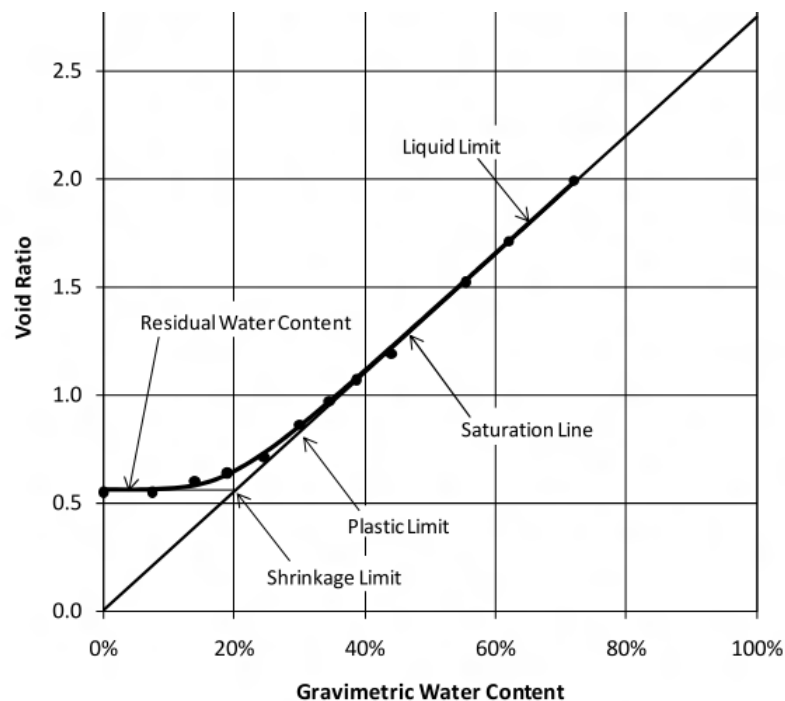


Figure 36: Demonstration of shrinkage characteristics clayey soil

5.9.1 Shrinkage curve equation

Equation 8 is a hyperbolic curve proposed by Fredlund et al.(1997, 2002) to fit to the shrinkage data.

$$e_w = a_{sh} \left[\frac{w^{c_{sh}}}{b^{c_{sh} a_{sh}}} + 1 \right]^{\left(\frac{1}{c_{sh}}\right)} \quad (8)$$

Where ,

a_{sh} is the minimum void ratio (e_{min})

b_{sh} is slope of the line of tangency in drying from saturated conditions

c_{sh} is inflection of the shrinkage curve, and w is gravimetric water content.

G_s is the specific gravity, and

S_r is the degree of saturation.

In this study, the void ratio-water content calculated by volume change during the suction measurements and shrinkage were obtained at different times. The shrinkage curves which describe the void ratio versus water content relationships between the sand-bentonite mixtures are shown in Figures 37-40.

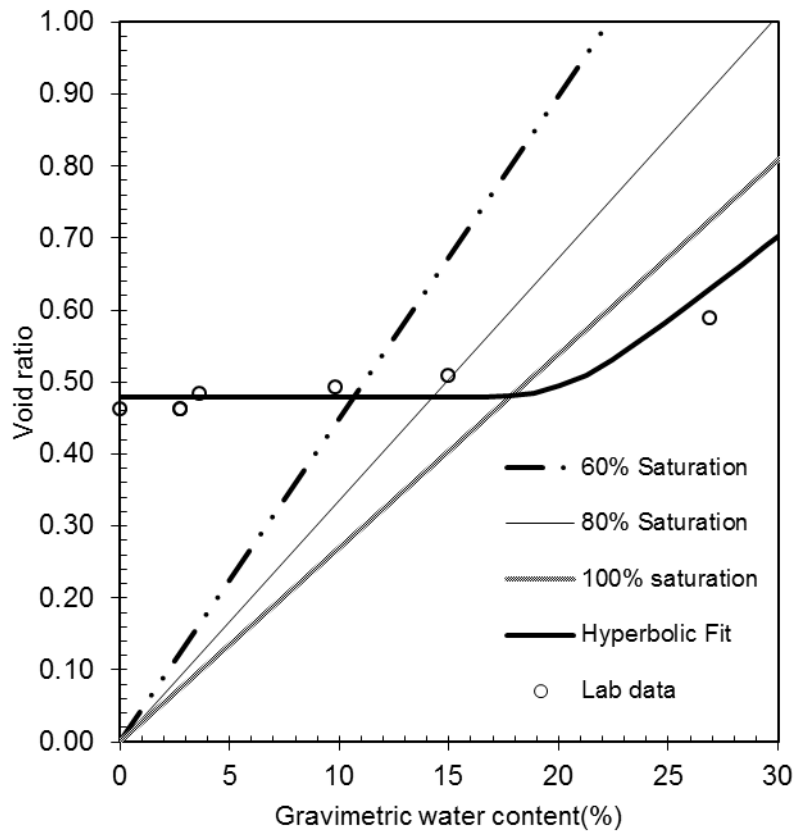


Figure 37: Shrinkage curve of sea sand +15% bentonite mixture

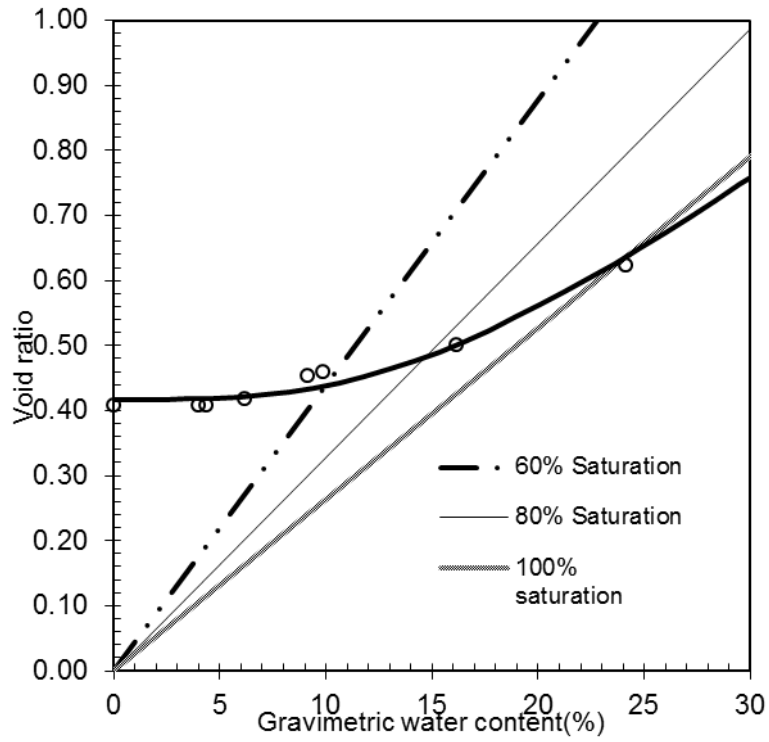


Figure 38: Shrinkage curve of sea sand +25% bentonite mixture

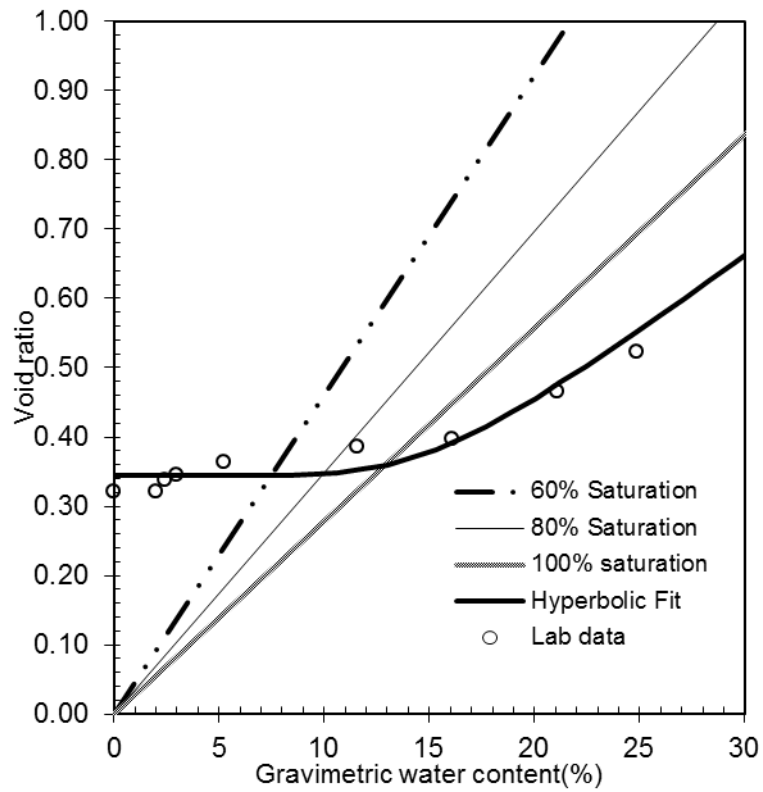


Figure 39: Shrinkage curve of crushed limestone sand +15% bentonite mixture

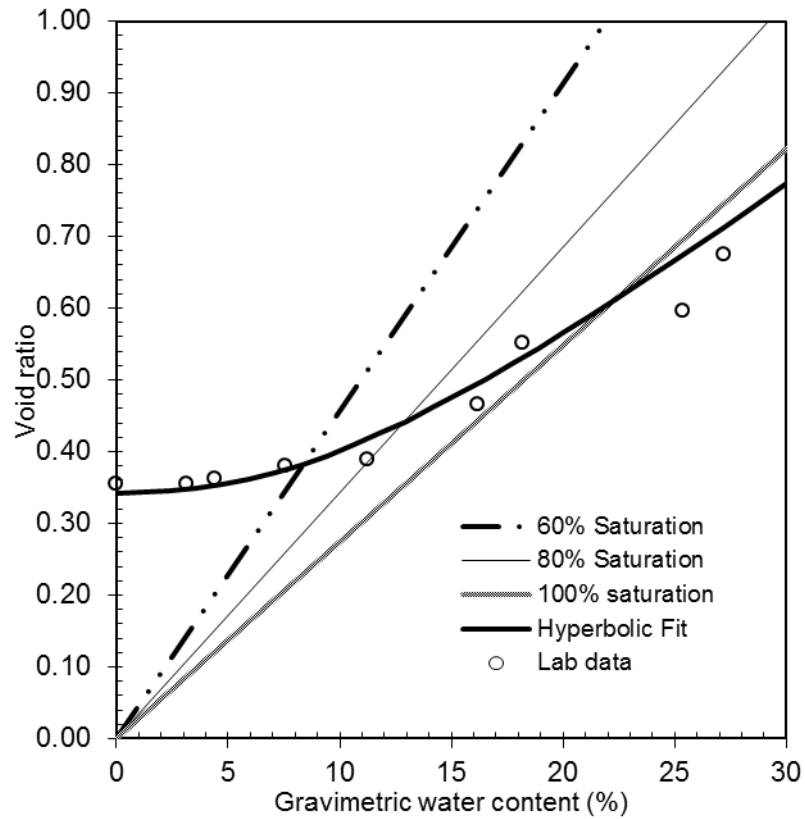


Figure 40: Shrinkage curve of crushed limestone sand +25% bentonite mixture

In sand–bentonite mixtures with increasing bentonite contents, shrinkage limit decreases in both sand types and therefore the volume change. The shrinkage curve supplies volumetric result for a soil as it desiccates and hence allows calculations of volumetric properties. For these calculations, shrinkage curve must be fit with the hyperbolic equation. The shrinkage curve parameters are specified in Table 17. The parameter a_{sh} , b_{sh} , c_{sh} represent the minimum void ratio (e_{min}), slope of the line of tangency in drying from saturated conditions, and inflection of the shrinkage curve reduction with increasing bentonite content in both sand type mixtures. No cracking and fractures are recorded in the mixtures with 15% bentonite, whereas cracks were observed in crushed sand with 25% bentonite.

Table 16: Shrinkage parameters calculated by Soil Vision software

Soil Type	a	b	c	R ²	shrinkage limit
Sea sand+15% bentonite	0.478	0.2045	16.669	0.9887	0.20
Sea sand+25% bentonite	0.417	0.1736	3.1807	0.9956	0.17
Crushed sand+15% bentonite	0.344	6.029	6.0292	0.9901	0.16
Crushed sand+25% bentonite	0.342	2.306	2.3065	0.9886	0.14

5.9.2 Three-Dimensional Shrinkage Test Results

Shrinkage test outcomes are described by plotting the average values of free shrinkage strains from two identical soil specimens. The volumetric, axial, and diametric strains versus time are given in Figure 41. The Figure displays percentage of shrinkage strains against elapsed time intervals. The samples were compacted at optimum water content, maximum dry unit weights, and left to swell completely. The majority of shrinkage in soils was recorded within the first 6 days (8000 min). Subsequent shrinkage rates were slow and no shrinking was recorded when samples were dried for more than 8 days (11000min). Volumetric, axial, and diametric stains increased with increasing bentonite content in both sand types. The crushed sand–bentonite mixtures have high shrinkage strains compared to sea sand–bentonite mixtures, and also contained shrinkage cracks.

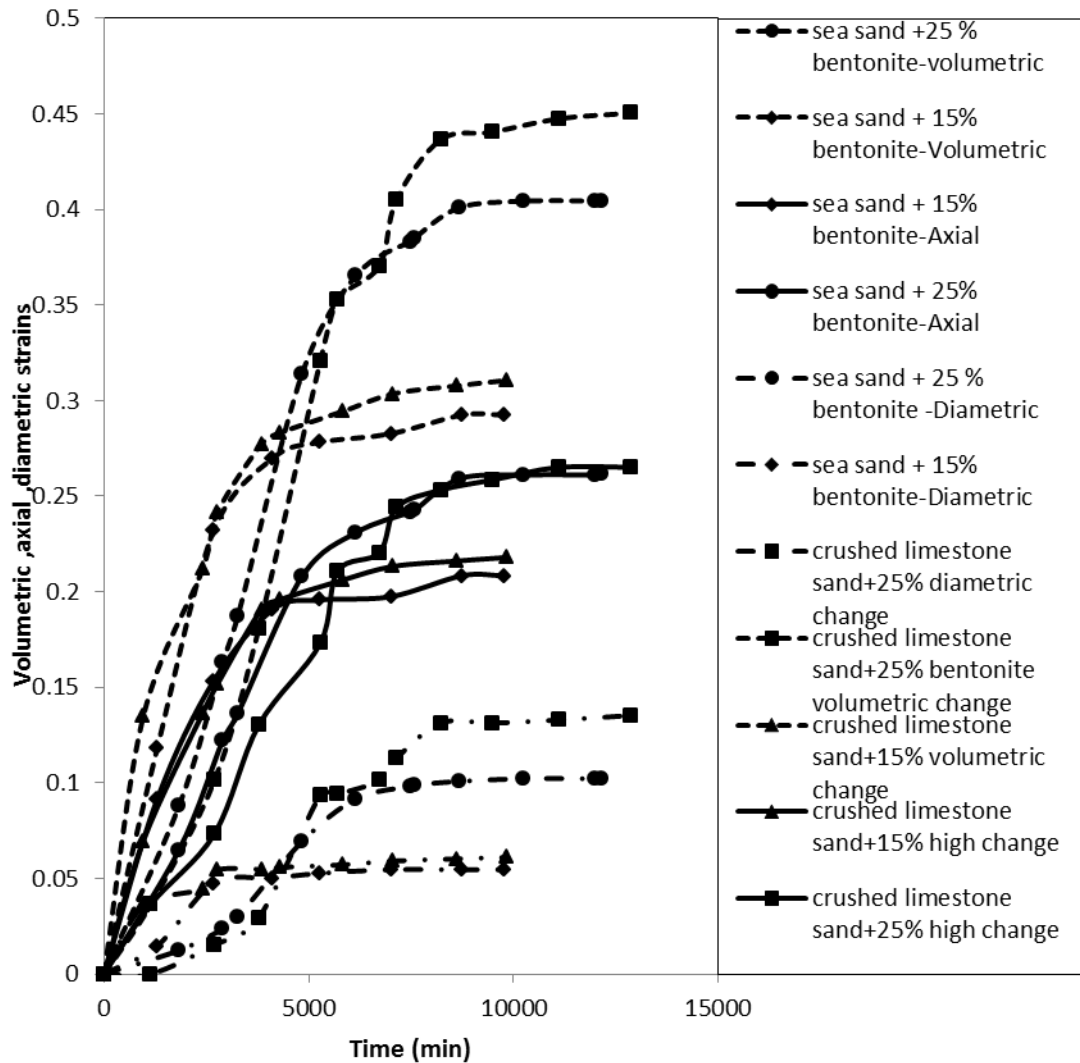


Figure 41: Volumetric, axial, diametric change curve

5.10 Ultrasonic Test

Table 17 displays the results of ultrasonic test for transit time and compression-velocity. Velocity of pulse in soil structure decreases if there are any obstacles such as air void, cracks or other faults. Initially sand-bentonite mixture samples were compacted at optimum water content and maximum dry unit weight. When the bentonite content increases in sand-bentonite mixtures, voids are filled with bentonite, the soil gets denser, hence compression velocity increases. This can be observed in Figure 45 with 25% bentonite content mixtures which have less air

voids, considerable increase in the compression wave. According to consolidation test, initial void ratio of crashed sand –bentonite samples is less than the sea sand–bentonite mixtures which have high compression velocity.

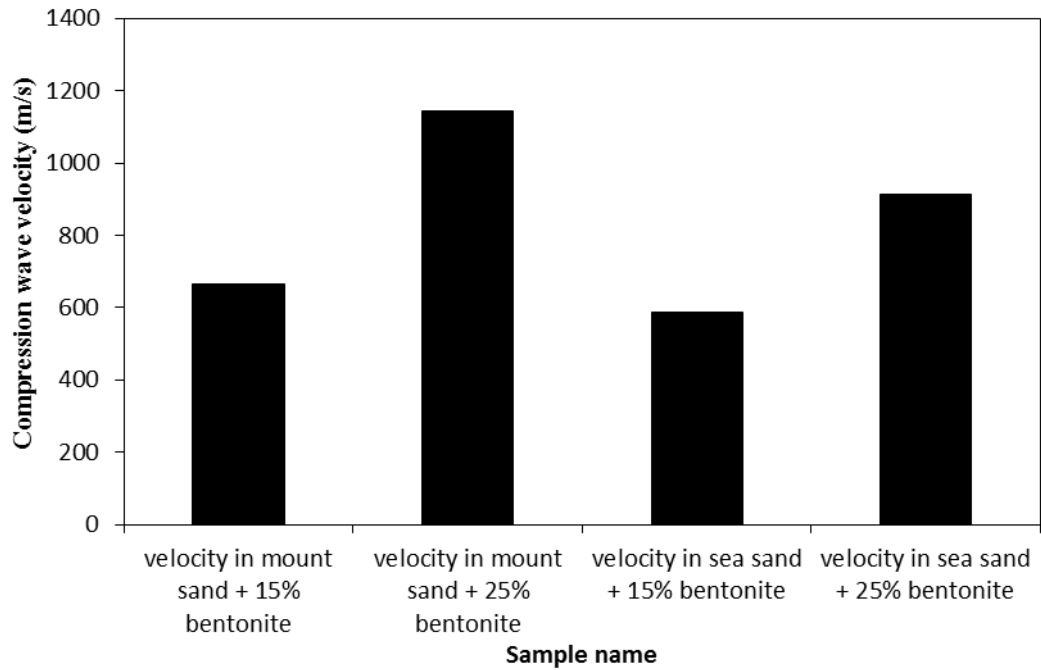


Figure 42: Compression wave velocity in as compacted wet soil (m/s)

Table 17: Compression wave velocity in different samples

Sample Name	$V_{wet}(m/s)$
Crushed sand + 15% bentonite	664
Crushed sand + 25% bentonite	1144
Sea sand + 15% bentonite	586
Sea sand + 25% bentonite	913

Chapter 6

CONCLUSIONS

An experimental research on the hydro-mechanical behavior of compacted sand-bentonite mixtures has been introduced. From the analysis of experimental data the following outcomes can be considered:

1. The bentonite content has important influence on the liquid and plastic limits. The liquid limit increases with an increase in bentonite content. The sand-bentonite mixture displays a clayey nature at relatively high water contents. In this case influence of the grading of the sand is diverse, liquid and plastic limit of sand in high amount of bentonite are greater than those of well-graded sand of the same content.
2. In dynamic compaction test, the mixtures of sea sand with addition of more bentonite to the mixture increases the maximum dry unit weight, but in crushed sand it decreases. In all of the samples increasing the bentonite content causes the reduction in optimum water content.
3. With increase in the bentonite content in sand-bentonite mixtures subjected to unconfined compression test, both the unconfined compressive strength and failure strain increase. The well graded sand has higher unconfined compressive strength value than the uniform graded sand.
4. In the one dimensional free swell test, the primary swelling of crushed limestone sand mixtures with bentonite increased with increment of the bentonite content.

The primary swelling ending time in both types of sand mixtures increased by increasing the bentonite content. Crushed limestone sand and bentonite mixture has high primary swelling compare to the sea sand-bentonite mixture.

5. Average results of consolidation tests presented that, the compressibility of sand-bentonite mixtures are increased with increase in the swelling and percentage of bentonite content. The swelling pressure increased with increasing bentonite content. The crushed limestone sand–bentonite mixtures display greater swelling pressures than other mixtures.
6. The saturated hydraulic conductivity reduces by increasing the bentonite content in both sand bentonite mixtures. The hydraulic conductivity of crushed limestone sand is lower than the sea sand.
7. The soil water characteristics curves and estimations declared that the air entry value attained by Fredlund and Xing (1994) model increased with the increasing content of bentonite into sea sand-bentonite mixture. The crushed limestone well-graded sand addition with 25% bentonite mixture, air entry value decreased with increase in the bentonite percentage. According to van Genuchten (1980) model, the air entry value decreases with increasing bentonite content in sea sand, and increases in crushed limestone sand. The residual water content obtained by Frudlund and Xing (1994) model increases by increment in the bentonite content in sea sand mixtures, whereas decreases in crushed limestone sand mixtures due to fracturing.
8. In low suction values, the sea and crushed limestone sand mixtures with 15% bentonite represent the high permeability in both loading pressures versus the mixtures with 25% bentonite which have low hydraulic conductivity value closer

upon desiccation. Sand bentonite mixtures have low hydraulic conductivity at high pressures.

9. The shrinkage test presented that in the sand–bentonite mixture with increasing bentonite content, shrinkage limit decreases in both sand types and therefore the volume change.
10. Volumetric, axial, and diametric strains increased with increase in the bentonite content in both sand type bentonite mixtures that show the high shrinkage behavior of bentonite particles. The crushed limestone sand–bentonite mixtures have high strains according to sea sand–bentonite mixtures.
11. In other to explain the compression velocity, with increase in the bentonite content in sand-bentonite mixtures, void ratios decrease, hence compression velocity increases in 25% bentonite content mixture.

REFERENCES

ASTM D2435 (1965). Standard Test Methods for One-Dimensional Consolidation Properties of Soils Using Incremental Loading. Annual Book of ASTM Standards, vol. 04.08, Soil and Rock; Building Stones, Sect. 4, ASTM, Philadelphia, PA.

ASTM D4546. (1980). *One-Dimensional Swell or Collapse of Cohesive Soils*. Annual Book of ASTM Standards, vol. 04.08, Soil and Rock; Building Stones, Sect. 4, ASTM, Philadelphia, PA.

Agus, S. S. (2005). An experimental study on hydro-mechanical characteristics of compacted bentonite-sand mixtures. Bauhaus-Universität Weimar, Germany.: PhD dissertation.

Agus, S. S., & Schanz, T. (2005b). Comparison of four methods for measuring total suction. *Vadose Zone Journal. Special section: Soil Water Sensing. Soil Science Society of America*, **4(4)**, 1087-1095.

Agus, S. S., & Schanz, T. (2005a). Swelling pressure and total suction of compacted Bentonite-sand mixtures. *Proceeding of International Conference on Problematic Soils, 1*, s. 61-70. North Cyprus.

Al-mukhtar, M., Qi, Y., Alcover, J. F., & Bergaya, F. (1999). Oedometric and water-retention behavior of highly compacted unsaturated smectites. *Canadian Geotechnical Journal*, **36**, 675-684.

ASTM. (1997). *Annual Book of Standards ,Soil and rock, ASTM International*. West Conshohocken. PA.

ASTM D2166-06 (1963). *Standard Test Method for Unconfined Compressive Strength of Cohesive Soil*. Annual Book of ASTM Standards, vol. 04.08, Soil and Rock;Building Stones, Sect. 4, ASTM, Philadelphia, PA.

ASTM D2845-95 (1969). *Standard Test Method for Laboratory Determination of Pulse Velocities and Ultrasonic Elastic Constants of Rock*. Annual Book of ASTM Standards, vol. 04.08, Soil and Rock;Building Stones, Sect. 4, ASTM, Philadelphia, PA.

ASTM D421-D422 (1935). *Standard Practice for Dry Preparation of Soil Samples for Particle-Size Analysis and Determination of Soil Constants*. Annual Book of ASTM Standards, vol. 04.08, Soil and Rock;Building Stones, Sect. 4, ASTM, Philadelphia, PA.

ASTM D4318-10 (1983) . *Standard Test Methods for Liquid Limit, Plastic Limit, and Plasticity Index of Soils*. Annual Book of ASTM Standards, vol. 04.08, Soil and Rock;Building Stones, Sect. 4, ASTM, Philadelphia, PA.

ASTM D5928-94 (1996). *Standard Test Method for Screening of Waste for Radioactivity*. Annual Book of ASTM Standards, vol. 04.08, Soil and Rock;Building Stones, Sect. 4, ASTM, Philadelphia, PA.

ASTM D698-7 (1942). *Standard Test Methods for Laboratory Compaction Characteristics of Soil Using Standard Effort (12 400 ft-lbf/ft³ (600 kN-m/m³)).* Annual Book of ASTM Standards, vol. 04.08, Soil and Rock; Building Stones, Sect. 4, ASTM, Philadelphia, PA.

ASTM D854 (1945). *Standard Test Methods for Specific Gravity of Soil Solids by Water Pycnometer.* Annual Book of ASTM Standards, vol. 04.08, Soil and Rock; Building Stones, Sect. 4, ASTM, Philadelphia, PA.

Barbour , S. L., & Fredlund, D. G. (1989). Mechanisms of osmotic flow and volume change in clay soils. *Canadian Geotechnical Journal*, 26, 551-562.

Benson, C. H., & Gribb, M. M. (1997). Measuring unsaturated hydraulic conductivity in the laboratory and field. *Unsaturated Soil Engineering Practice Geotechnical Special Publication*, 68. ASCE, 0-7844-0259-0, 113–168.

Bolt, G. H. (1956). Physico-chemical analysis of the compressibility of pure clays. *Géotechnique*, 6(2), 82-93.

Bradbury, M. H., & Baeyens, B. (2003). Porewater chemistry in compacted re-saturated MX-80 bentonite. *Journal of Contaminant Hydrology, Elsevier*. 61, 329-338.

Brandl, H. (1992). Mineral liners for hazardous waste containment. *Geotechnique*, 42, 57-65.

Brooks, R. H., & Corey, A. T. (1966). Properties of porous media affecting fluid flow. *Journal of the Irrigation and Drainage Division, ASCE*, **92(IR2)**, 61–89.

Croney, D., & Coleman, J. D. (1961). Pore pressure and suction in soil. *In Proceedings of Conference on Pore Pressure and Suction in Soils* (s. 31-37). London: Butterworths.

Daniel, D. E. (1982). Measurement of hydraulic conductivity of unsaturated soils with thermocouple psychrometers. *Soil Science Society of America Journal* .**46**, 1125–1129.

Daniel, D. E., & Choi, H. (1999). *Hydraulic conductivity evaluation of vertical barrier walls*. Reston, Virginia: Geo-Engineering for Underground Facilities, GSP No. **90**, ASCE.

D'Appolonia, D. J. (1980). Soil-bentonite slurry trench cutoffs. *Journal of Geotechnical Engineering, ASCE*, **106(4)**, 399 - 417.

Das, B. M. (2006). *Principles of Geotechnical Engineering*. Boston: PWS-Kent.

Delage , P., & Graham, J. (1996). Mechanical behaviour of unsaturated soils: Understanding the behaviour of unsaturated soils requires reliable conceptual models. *In Proceedings of the 1st International Conference on Unsaturated Soils (UNSAT 95)*, (s. 1223-1256). Paris, France.

Delage, P. (2007). Microstructure features in the behaviour of engineered barriers for nuclear waste disposal. Proc. 2nd International Conference: Mechanics of Unsaturated Soils (Ed. Tom Schanz). **1**, s. 11-32. Weimar, Germany.: Springer proceedings in physics.

Delage, P., & Cui, Y. J. (2008). An evaluation of the osmotic method of controlling suction. *Geomechanics and Geoengineering: An International Journal*,**3(1)**, 1-11.

Dixon, D. A. (2000). Porewater salinity and the development of swelling pressure in bentonite-based buffer and backfill materials. Helsinki,Finland: POSIVA Report 2000-04. Posiva Oy.

El Sohby, M. A., & Rabba, E. A. (1981). Some factors affecting swelling of clayey soils. *Geotechnical Engineering Journal, SEAGS*, 19 – 39.

Evans, J. C. (1991). *Geotechnics of hazardous waste control systems*. New York: Foundation Engineering Handbook, 2nd ed., H.-Y. Fang, ed.,Chapman and Hall.

Evans, J. C. (1994). *Hydraulic conductivity of vertical cutoff walls*. Philadelphia: Hydraulic Conductivity and Waste Contaminant Transport in Soil, ASTM STP 1142, ASTM.

Evans, J. C., Costa, M. J., & Cooley, B. (1995). Slurry wall performance. *Proc., Progress in Geotechnical Engineering Practice, ASCE and PENNDOT, Hershey, Pa.*

Filz, G. M. (1996). Consolidation stresses in soil-bentonite backfilled trenches. *Proc. 2 nd Int. Congress on Environmental Geotechnics*, (s. 497-502). Osaka, Japan.

Filz, G. M., Henry, L. B., Heslin, G. M., & Davidson, R. R. (2001). Determining hydraulic conductivity of soil-bentonite using the API filter press. *Geotechnical Testing Journal, ASTM*, **24(1)**, 61-71.

Filz, G. M., Baxter, D. Y., Bentler, D. J., & Davidson, R. R. (1999). Ground deformation adjacent to a soil-bentonite cutoff wall. *Geo-Engineering for Underground Facilities, GSP No. 90*, ASCE, Reston VA, 121-139.

Fleureau, J. M., Verbrugge, J. C., Huergo, P. J., Correia, A. G., & Kheirbek-Saoud, S. (2002). Aspects of the behaviour of compacted clayey soils on drying and wetting paths. *Canadian Geotechnical Journal*, **39**, 1341-1357.

Fredlund, D. G., & Xin, A. (1994). Equations for the soil-water characteristic curve. *Canadian Geotechnical Journal*, **31**, 521-532.

Fredlund, D. G., & Rahardjo, H. (1993). *Soil mechanics for unsaturated soils*. Canada: John Willey & Son.

Gens, A., Alonso, E. E., Suriol, J., & Lloret, A. (1995). Effect of the structure and volumetric behaviour of a compacted soil. *Proceedings of the first International Conference on unsaturated soils*, **1**, s. 83-88. Paris, France.

Gens, & A. and Alonso, E. (1992). A framework for the behaviour of expansive clays. *Canadian Geotechnical Journal*, **33**, 11-22.

Head, K. H. (1992). *Manual of Soil Laboratory Testing* (Second b). London: Pentech Press.

Ito, H., & Komine, H. (2008). Dynamic compaction properties of bentonite-based materials. *Engineering Geology*, **98**, 133–143.

Khoury, M. A., Fayad, P. H., & Ladd, R. S. (1992). Design, construction, and performance of a soil-bentonite cutoff wall constructed in two stages. *Slurry Walls: Design, Construction, and Quality Control, ASTM STP 1129*, 289-308.

Komine, H., & Ogata, N. (2003). New equations for swelling characteristics of bentonite-based buffer materials. *Canadian Geotechnical Journal*. **40**, 460-475.

Kraus, JF, C.H., Erikson, A.E., Chamberlain, et al. (1997). Freeze-thaw cycling and hydraulic conductivity of bentonite barriers. *Journal of Geotechnical Engineering*. ASCE. Vol **123**. No 3, 229-238.

Kumar, S., & Yong, W. L. (2002). Effect of Bentonite on Compacted Clay Landfill Barriers. *J. Soil and Sediment Contamination*, **11(1)**, 71-89.

Kumar, S., & Yong, W. L. (2002). Effect of Bentonite on Compacted Clay Landfill Barriers. *J. Soil and Sediment Contamination*, **11(1)**, 71-89.

Laird , D. A. (2006). Influence of layer charge on swelling of smectites. *Applied Clay Science, Elsevier*. **34**, 74-87.

Lambe, T. W. (1960). Structure of compacted clay. *Transaction Am. Soc. Civ. Eng.* **125**, 682-705.

Leong, E. C., & Rahardjo, H. (1997). Review of soil-water characteristic curve equations. *Journal of Geotechnical and Geo-environmental Engineering, ASCE*, **123(12)**, 1106–1117.

Ltd, S. S. (1992). User's Guide- A Knowledge Based System for Soil Properties, Version 2.0, Saskatoon, Canada.

Madsen, F. T., & Müller-Vonmoos , M. (1989). The swelling behaviour of clays. *Applied Clay Science, Elsevier*. **4**, 143-156.

Marinho, F. M. (2005). Nature of soil-water characteristic curve for plastic soils. *Journal of Geotechnical and Geoenvironmental Engineering , ASCE*. **131 (5)**, 654-661.

Mathew, P. k., & Rao, S. N. (1997). Influence of cations on compressibility behavior of acations marine clay. *Technical Note, Journal of Geotechnical and Geoenvironmental Engineering, ASCE*, Vol.**123 (11)**, 1071-1073.

Mesri, G., Pakbaz, M. C., & Cepeda-Diaz, A. F. (1994). Meaning, measurement and field application of swelling pressure of clay shales. *Geotechnique*, **44 (1)**, 129-145.

Mitchell, J. K. (1993). *Fundamentals of Soil Behavior*. NY: 2nd Edition. John Wiley & Sons Inc.

Mualem, Y. (1986). A new model for predicting the hydraulic conductivity of unsaturated porous media. *Water Resources Research*, **12**, 513-522.

Ng, C. W., & Pang, Y. W. (2000). Influence of the stress state on soil water characteristics and slope stability. *ASCE. Journal of Geotechnical and Geo-Environmental Engineering*, vol.**126**, 157-166.

Pusch, R., Karliland, O., & Hokmark, H. (1990). *GMM-a general microstructural model for qualitative and quantitative studies of smectite clays*. Stockholm, Sweden: SKB Technical Report 90-43.

Pusch, R. (1979). Highly compacted sodium bentonite for isolating rock-deposited radioactive waste products. *Nuclear Technology* 45, 153-157.

Pusch, R. (2001). *The microstructure of MX-80 clay with respect to its bulk physical properties under different environmental conditions*. Stockholm, Sweden: SKB Technical Report, TR-01-08. The Swedish Nuclear Fuel and Waste Management Company (SKB).

Pusch, R., & Yong, R. (2003). Water saturation and retention of hydrophilic clay buffer-microstructural aspects. *Applied Clay Science, Elsevier*.**23**, 61-68.

Richards, B. G. (1965). Measurement of the free energy of soil moisture by the psychrometric technique using thermistors. *In moisture equilibria and moisture change in beneath covered area (Eds. G.D. Aitchison) soils* (s. 39-46). Sydney, Australia: Butterworth & Co. Ltd.

Ridely, A. M. (1995). Discussion on " Laboratory filter paper suction measurements " by Sandra L. Houston, William N. Houston , and Anne-Marie Wanger. *Geotechnical Testing Journal ,GTJODJ*, **18**, 391-396.

Ross, C.S., & Hendricks, S. B. (1945). Minerals of the montmorillonite group – Their origin and relation to soils and clays. *US Geological Survey Professional Paper 205-B*, 79.

Rossi, C., & Nimmo, J. R. (1994). Modeling of soil water retention from saturation to oven dryness. *Water Resources Research*, **30(3)**, 701–708.

Saiyouri, N., Tessier, D., & Hicher, P. Y. (2004). Experimental study of swelling in unsaturated . *compacted clayss*, **39** , 469-479.

Schanz, T., & Tripathy , S. (2005). Soil water characteristic curves of clays from physico-chemical concepts. H. Bilsel, & Z. Nalbantoglu (Dü.), *Proceeding of International Conference on Problematic Soils içinde, 1*, s. 219-228. North Cyprus.

Schneider, J. (1994). *Soil bentonite cut-off walls*. Singleton, New South Wales: Australian National Committee on Large Dams.

Sridharan, A., & Jayadeva, M. S. (1982). Double layer theory and compressibility of clays. *Geotechnique*, **32**(2), 133-144.

Stewart, D. I., Studds, P. G., & Cousens, T. W. (2003). The factors controlling the engineering properties of bentonite-enhanced sand. *Applied Clay Science*, **23** (1-4), 97-110.

Tessier, D., Dardaine, M., Beaumont, A., & Jaunet, A. M. (1998). Swelling pressure and microstructure of an activated swelling clay with temperature. *Clay Minerals*, **33**, 255-267.

Toll, D. G. (1995). A conceptual model for the drying and wetting soil. *Proceedings of First International Conference on Unsaturated Soils*, **2**, s. 805-810. Balkema.

Tripathy, S., Schanz, T., & Sridharan, A. (2004). Swelling pressures of compacted bentonites from diffuse double layer theory. *Canadian Geotechnical Journal*, **41**, 437-450.

van Genuchten, M. T. (1980). A closed-form equation for predicting the hydraulic conductivity of unsaturated soils. *Soil Science Society of America Journal*, **44**, 892-898.

Van Olphen, H. (1963). *An introduction to clay colloid chemistry*. New York and London: Interscience.

- Vanapalli, S. K., Fredlund, D. G., & Pufahl, D. E. (1999). Influence of soil structure and stress history on the soil-water characteristics of a compacted till. *Geotechnique*, **49**, 143-159.
- Villar, M. V., & Lloret, A. (2004). Influence of temperature on the hydro-mechanical behaviour of a compacted bentonite. *Applied Clay Science, Elsevier*, **26**, 337-350.
- Villar, M.V., & Lloret, A. (2008). Influence of dry density and water content on the swelling. *Applied Clay Science*, **39**, 38–49.
- Wersin, P., Johnson, L.H., & McKinley, I. G. (2007). Performance of the bentonite barrier at temperatures beyond 100 °C: a critical review. *Physics and Chemistry of the Earth*, **32**, 780-788.
- Yahia-Aissa, M., Delage, P., & Cui, Y. J. (2000). Volume change behavior of a dense compacted swelling clay under stress and suction change. *Experimental evidence and theoretical approaches in unsaturated soil. Trento 10-12 April.*, 65-74.
- Ye, M. W., Schaze, S., Qian, L. X., Wang, J., & Arifin. (2007). Characteristics of swelling pressure of densely compacted gaomiaozhi bentonite GMZ01. *Chinese Journal of Rock Mechanics and Engineering* **26**, 3861–3865 (in Chinese).
- Yong, R. N. (1999). Soil suction and soil-water potentials in swelling clays in engineered clay barriers. *Engineering Geology, Elsevier*, **54**, 3-13.

Yong, R.N., BOONSINSUK, & P. WONG, G. (1986). Formulation of backfill material for a nuclear fuel waste disposal vault. *Can. Geotech. J.* **23**, 216-228.